THE DESIGN AND CONSTRUCTION
OF A
TEA MOLECULAR NITROGEN LASER SYSTEM

by

ADNAN KURT

B.Sc. in Electrical Engineering, Bogazici University, 1984.

Submitted to the Institute for Graduate Studies in
Science and Engineering in Partial Fulfilment for the
Requirements of the Degree of

MASTER OF SCIENCE

in

PHYSICS

BOGAZICI UNIVERSITY

January 1988

DESIGN AND CONSTRUCTION OF A TEA NITROGEN LASER

APPROVED BY

Yrd.Doc.Dr. A.J.WETHERILT ....
(Thesis Supervisor)

Dr. A.EASTOP ....

Prof.Dr. O.SAYGIN

DATE OF APPROVAL 1.2.1988.

ACKNOWLEDGEMENTS

I would like to express my deepest gratitude to **A.J.Wetherilt**, my thesis supervisor. With his guidance and valuable support this work has been accomplished.

I have been encouraged and shown the way by **R.Emrich**, who spent an important amount of his valuable time to help me. **K.Kumcu** made the arrangements for some experiments to be conducted at TBTAK, and also supplied me with his experience and knowledge on dye lasers. Also he supplied several hard-to-buy devices. **E.Sözen** coated the dielectric mirrors. **K.Doğaç** made the mechanical machining and his skill and hard working made it possible. **H.Özbal** let me use his nitrogen gas. I appreciate their cooperative attitude and kindness.

My beloved friends, **M.Artun, C.Koçak, C.Palanduz, K.Pinçe, H.Yapar, İ.Canata, M.Güner, D.Kalfaoğlu, F.C.Atay** have supplied materials, devices, helped in drawings and during the writing, and I am sure that without their support this work would really be very hard to complete.

I would also like to state my thanks to the members of the Physics Department for their aid and support during my studies.

ABSTRACT

In this study the design and construction of a molecular nitrogen laser intended as a pump source for a dye laser system is presented. This laser emits radiation at a wavelength of 337.1 nanometers and uses Blumlein switching to achieve fast (~ a few nanosecond width) and high peak power (~ a few hundred kilowatts) pulses. It operates using atmospheric pressure nitrogen with a cavity length of ten centimeters.

The incorporation of this laser into a wavelength tunable, pumped dye laser system is outlined. Methods for studying fast optical pulses are given.

ÖZETÇE

Bu çalışmada, organik boya lazerlerinin pompalanması amacıyla, atmosfer basıncında çalışan, enine uyarmalı bir azot lazerinin tasarımı ve yapımı işlenmiştir.

Fiziksel dizgelerin deneysel çözümlenmesinde, bilimsel disiplinlerin çoğu, gereksinimlere göre uyarlanmış parametrelerde hızlı uyarıcı mekanizmalar kullanırlar.

Boya lazerinin sağladığı değişken renkli hızlı ışık darbeleri, katıhal fiziğinde değişik enerjilerde uyarımlar yaratmada, plazmalarda şok dalgaları ölçümünde, optik lif çalışmalarında yayınım özelliklerini bulmada, foton etkileşimlerinde kullanılırken, kimyada moleküller arası enerji aktarımında, ışıkla ayrışmada, yük aktarımında kullanılır. Biyolojide ise fotosentez çalışmaları, hemoglobin, rhodopsin ve DNA ile ilgili çalışmalarda önemli bir araçtır.

Bu tezde sözü geçen azot lazeri, yarı iletken fiziğinde sürdürülen çalışmalarda, doğrusal olmayan optik ve çok hızlı görüngülerin çözümlenmesi çalışmalarında kullanılmak üzere bir boya lazerini pompalamak için tasarlanmıştır.

Çalışma süresi içerisinde azot lazerinin yapımı tamamlanıp, boya çözeltileri içerisinde ışıldama ve lazer etkisinin gözlemlenmesine çalışıldı. Azot gazındaki lazer ışıldamasının darbe genişliği, ışık şiddeti, dağılması gibi bir takım fiziksel parametrelerin kuramsal ve deneysel kestrimleri için çalışmalar yapıldı.

Ölçüm aygıtlarının eksikliği nedeniyle fiziksel parametrelerle ilgili kesin bilgiler verilmemekle birlikte, bu çalışmada, enine uyarılan azot lazerinin tasarımı ve yapımıyla ilgili bilgi ve genel fiziksel koşullara ilişkin gözlemlerle, hızlı darbelerin ölçülmesi yöntemleri ve lazer ışıması için gerekli koşullarla ilgili bilgi verilmiştir.

Table of CONTENTS

LIST of FIGURES

I. INTRODUCTION

Lasing action in molecular nitrogen was first reported in 1963 by Heard (1).The lasing action occured between the $C^3\pi_u$ and $B^3\pi_g$ bands transition at a measured wavelength of 337.1 nm. Following this discovery, the lasing and excitation mechanisms were investigated by several workers (2,3,4,5). Generally the lasers constructed by these workers operated at low nitrogen pressures (between about 30 to 100 torr) and often used the technique of **Blumlein switching** (6,7,8,9,10) to obtain fast, high current pulses (typically 40 KA over 1 ns period) through a discharge region, populating excited $C^3\pi_u$ states by direct electron impact.

Theoretical calculations by **Gerry,Ali et.al.** (11,12,13) and experimental studies showed that the optimum working pressure should be about 20 to 30 torr as a result of the cooling of electrons at higher pressures (12,14) and the formation of erratic discharges at higher voltages. The advent of photopreionization techniques by **Bergmann, Hasson** and

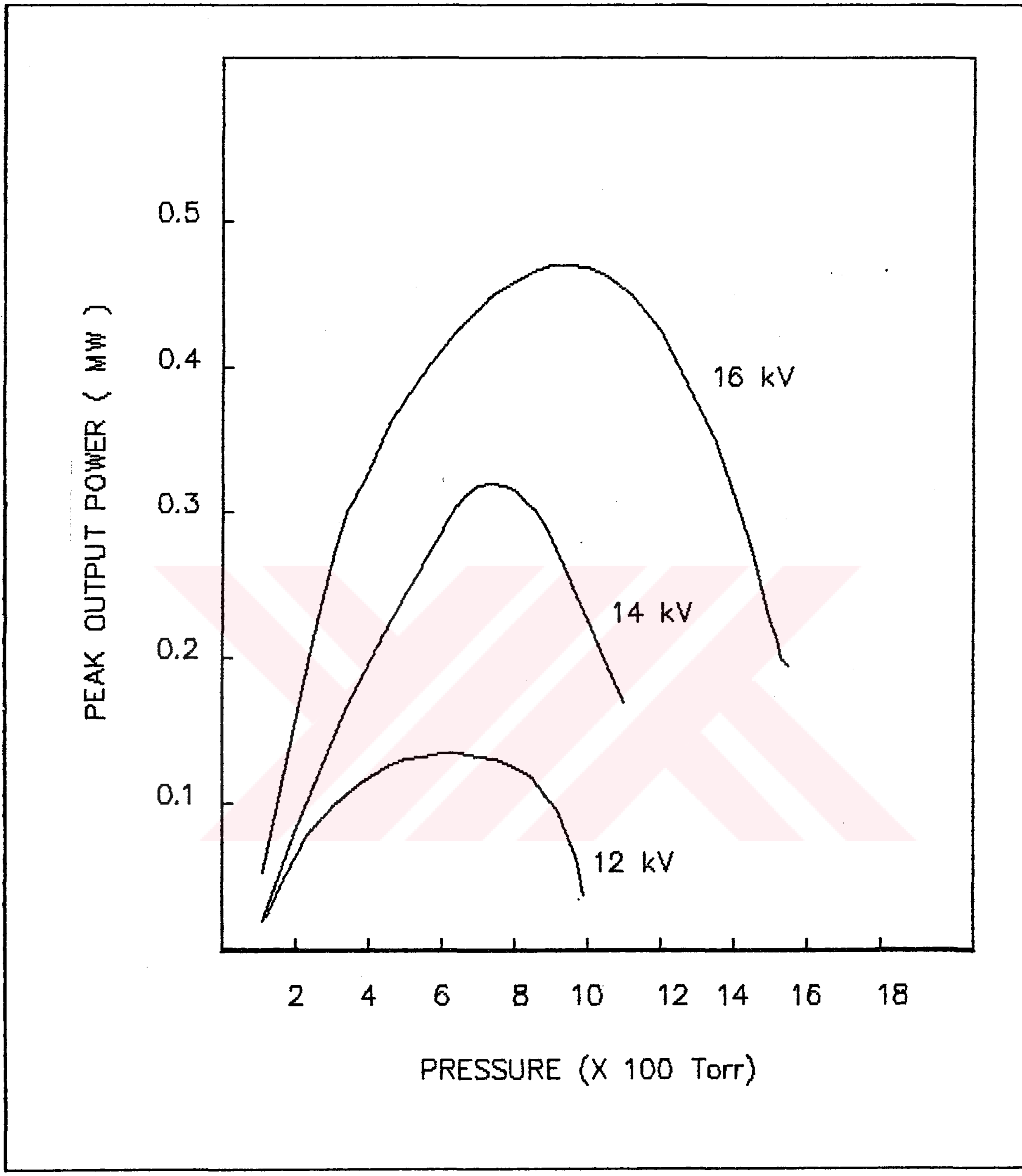

FIG 1: PEAK LASER POWER DENSITY
vs
NITROGEN PRESSURE for
VARIOUS CHARGING VOLTAGES

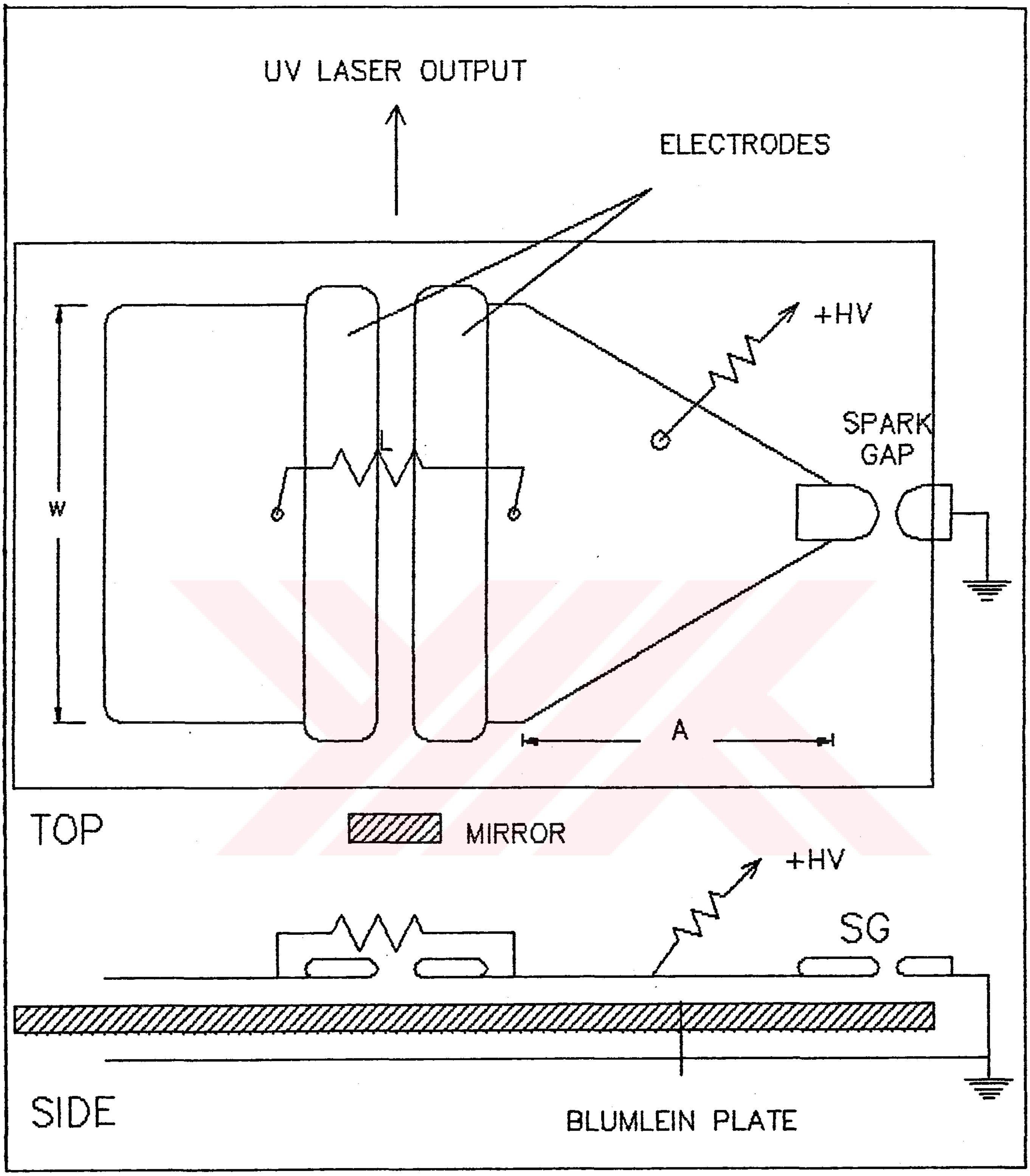

FIG 2: GENERAL STRUCTURE
for
TEA NITROGEN LASERS
with
Blumlein Excitation and Spark Gap Switching

others (15,16,17) in the 1970s, where UV radiation from a corona discharge initiates the lasing transition, enabled much higher pressures of nitrogen to be used thus increasing the output power of the system in some cases by many orders of magnitude (18,19,20) (figure 1).

The very high gain of the high pressure N_2 lasers allowed the physical size of the lasing cavity to be reduced to permit much more compact designs. Laser cavities of only a few cubic millimeters in volume have been reported with output powers of several hundred kilowatts (20). The gain of these systems is generally such that mirrors are not necessary for the production of pulses in contrast to virtually every other type of laser. The general structure for the transversely excited gas lasers is shown in figure 2.

The use of a Fabry-Perot cavity with N_2 lasers does not significantly change the low coherence (several millimeters (23)) and high beam divergence (10 mradian (21,22)) because of the short photon lifetime inside the cavity. The effects of low coherency and poor divergence are generally minimized by using two coupled lasers in a configuration where one is used as an oscillator and the other as an amplifier (24). The N_2 laser is frequently used in conjunction with dye lasers, as the combination of high output power, short wavelength, short pulse duration, typical of the N_2 laser, create excellent pumping sources for dye lasers. There have been several methods developed for exciting dye solutions, the simplest one uses N_2 laser pulses to drive a dye solution in a UV transparent cuvette into the superradiant mode (8,24,25,26,). Generally an optical cavity is used to obtain more coherent and monochromatic output and to improve the system gain. A unique feature of dye lasers is that the output wavelength can be continuously varied over a wide range if the cavity includes a tuning mechanism such as a prism or grating (27,28,29).

In order to obtain shorter (<500 ps (30)), high power pulses, **passive Q-switching** is often employed. It has been shown that the use of a Q-switch can increase the dye laser gain by a factor of six.

Experimental systems and techniques used are covered extensively in the literature. There are many references to the physics of dye laser systems and to their lasing and excitation mechanisms. However, the theoretical foundation of N_2 laser was first developed by **Gerry, Leonard and Ali** (11,13).

These authors present the system equations and several parametric solutions after a number of approximations (12). The theoretical basis for all subsequent N_2 laser systems refer to this work.

A second formalism that could be related to the physics of N_2 lasers, treats the laser as a **"cooperative system"** and predicts the phenomenon of **superradiance.** **Dicke** first dicovered the superradiant effect (33,34,35) which forms the basis for all subsequent work. Using this approach **Arecchi, Bonifacio** and others (36,37,38,3940,41) extended the *limited scope of Dicke's original superradiant* model, and were able to calculate threshold conditions, radiation modes, pulse shapes and and other physical parameters.

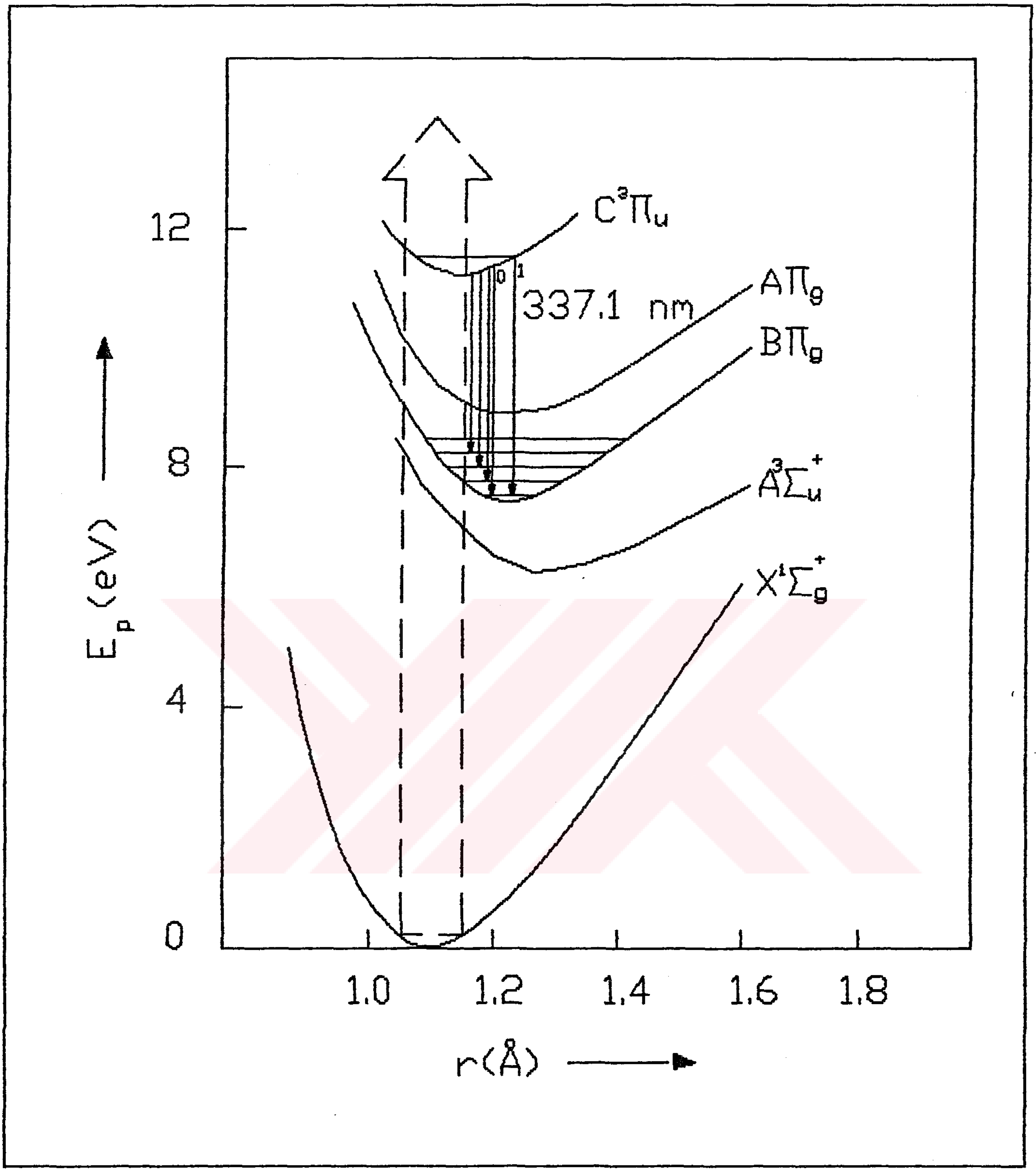

FIG 3: Energy level diagram of nitrogen molecule,
r = internuclear distance
Ep = potential energy

II. DESIGN RULES

At low nitrogen pressures (less than 20 kPa) it is reported that specific output powers of the order of 50 GWm^{-3} have been attained (22,42), with conventional nitrogen lasers. However developing high pressure operation, **von Bergmann** et.al. reported (43,48) that yields of up to 1 TWm^{-3} were probable, using photoionization-stabilized glow discharge systems. The specific output powers made the construction of compact N_2 lasers possible.

2.1 General Considerations

The mechanism of the laser action is unusual since the lifetime of the upper $C^3\pi_u$ level (with lifetime < 40 ns) is much shorter than that of the lower $B^3\pi_g$ level (with 6µs lifetime).The energy level diagram for the

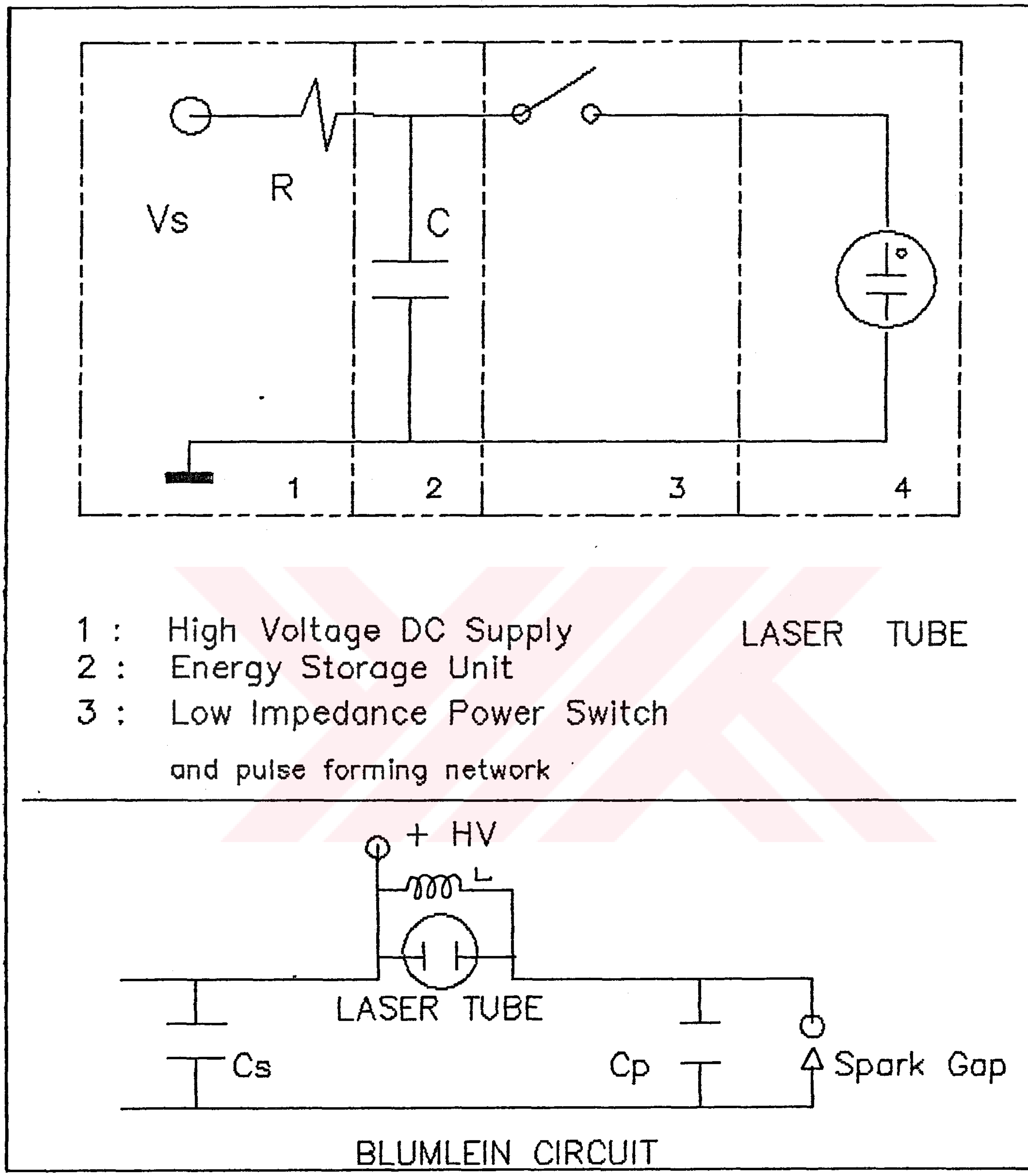

FIG 4: ELECTRICAL MODELS
for
TEA NITROGEN LASER

nitrogen molecule is given in figure 3. Population inversion can only be achieved because the electron excitation cross-section is about twice as large for the upper as for the lower level (44). The most important consideration is that the pumping rate should be faster than the $C^3 \pi_u$ lifetime,so that an inversion of the population can be attained before spontaneous emission, which causes significant depopulation to the lower levels.At higher fill-pressures,the lifetime of the upper laser level is even shorter which makes it more difficult to establish the inversion threshold.

The laser requires large current densities ($>$ 1kAcm^{-2} (8,45)) and a high electron temperature ($\geq$ 5 eV (46,13)).The required rate of current rise, of the order of 10^{12} A/sec, places severe restrictions on the inductance and resistance of the entire discharge circuit (figure 4) (6).To minimize these parameters, instead of energy storage elements, transmission lines are used and connected directly to the laser tube. In order to use it also as a pulse forming network, a high speed switch is utilized to allow the line to charge to the necessary potential before discharging through the gas.

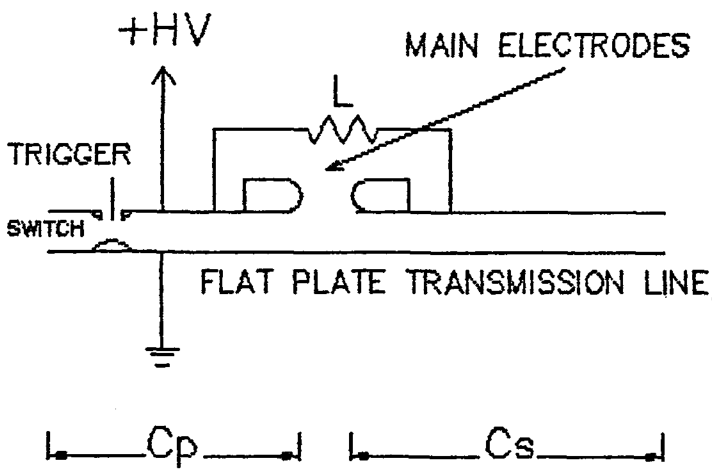

FIG 5: LASER DISCHARGE CIRCUITRY
STRUCTURE of TRIGGERING
and
PULSE FORMING & ENERGY STORAGE CAPACITORS

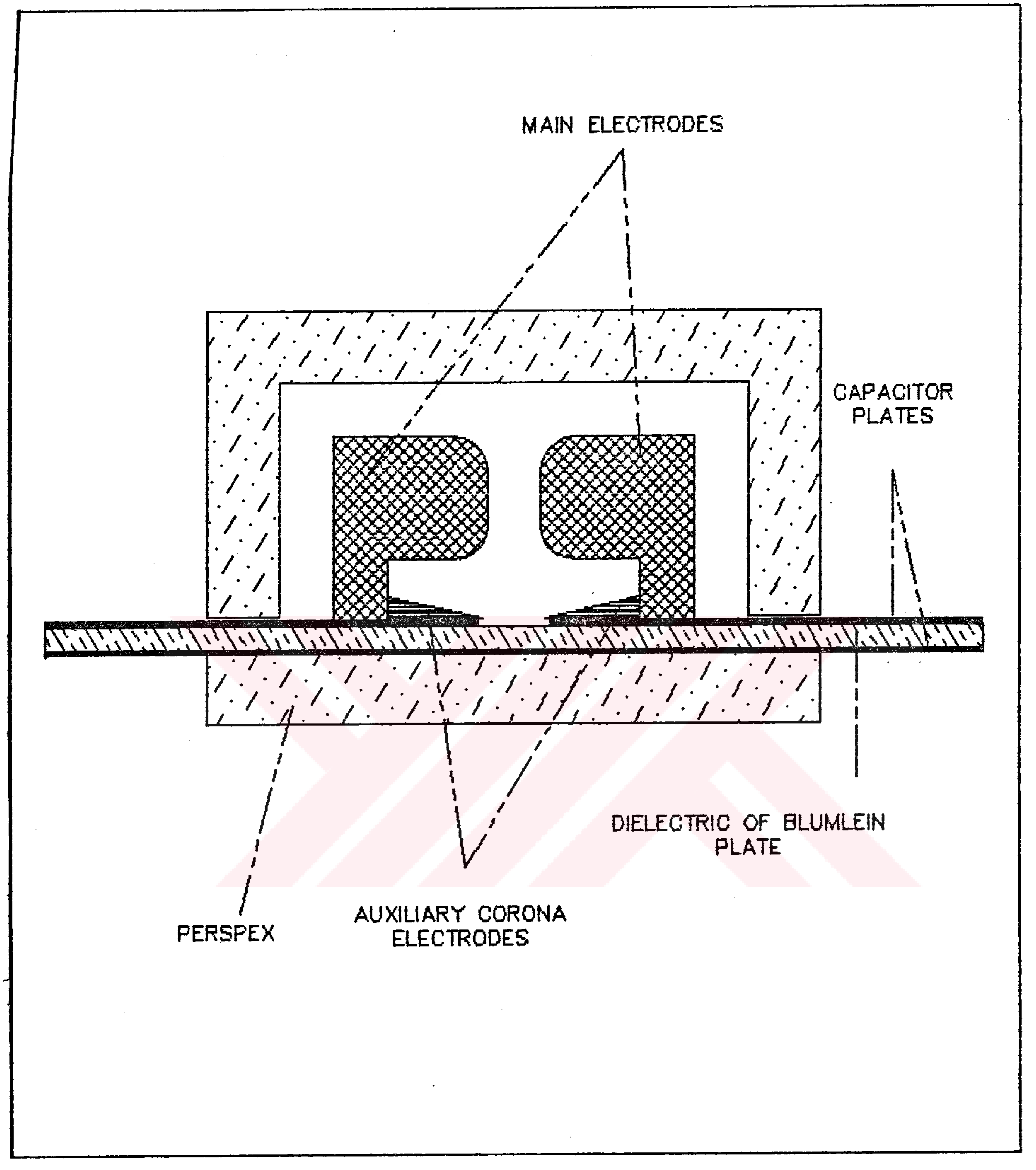

FIG 6: NITROGEN LASER PLASMA CHAMBER and ELECTRODE CONFIGURATIONS

The common way of high-speed high voltage pulse forming is to use the **Blumlein effect,** where the transmission line is used for two separate purposes of energy storage and pulse formation (figure 5). The energy storage capacitor C_s and pulse forming capacitor C_p are charged to the same potential via an inductor L connected in between them. In parallel to the inductor there is the laser discharge cavity where the ionization occurs. By the breakdown of the sparkgap at the threshold voltage a high potential difference appears between the electrodes or across the inductor. Given a sufficiently high rate of current rise ($\approx 10^{12}$ A/sec) the stimulated emission in the transverse direction is obtained. The problem with this system is to overcome the erratic discharges and arc formation at high pressures. The method of solution is to use a photopreionization technique (20,47,49,50,51) where the gas in the discharge volume is ionized with the UV photon emission from the corona discharge formed over the surface of dielectric between the auxiliary electrodes (figure 6).

2.2 Transmission Line Analysis

The characteristic impedance of the system determines the current through the cavity, the current risetime therefore is a critical parameter for succesful operation and output power. The system, without impedance matching would result both in pulse broadening because of reflected electromagnetic waves in the stripline and power reduction (44). Breakdown of the spark gap switches the pulse-forming plate, previously charged to V_o by the high voltage supply, to the ground. A ground-going pulse of amplitude V_o propagates along the stripline of impedance Z_a towards the cavity. At the end of the cavity the pulse sees a total impedance of Z_b+Z_L. Transmission line analysis gives, for the reflected and transmitted current pulses:

$$I_r = \frac{Z_b+Z_L-Z_a}{Z_b+Z_L+Z_a} \quad I_i \qquad (2.1)$$

$$I_t = I_i - I_r = \frac{2Z_a}{Z_a+Z_b+Z_L} I_i \qquad (2.2)$$

where I_i, I_r, I_t are incident, reflected and transmitted currents respectively and Z_a, Z_b, Z_L are line forming, storage and plasma impedances in the given order (in figure 2, the impedances of circuit elements are shown).

The reflected pulse propagating towards the spark gap reverses its polarity, since it is terminated by a shorted spark gap. The pulse that was transmitted to the energy storage plates does not change its polarity since it is terminated by an open circuit.For $Z_L = 2Z_a = 2Z_b$,all the succeeding reflections will be matched and cancelled, giving a total pulse of duration $2T_o$, where $T_o = a/\nu$. If $Z_L << Z_a = Z_b$,then the reflected pulse amplitude is negligible with giving a pulse of duration T_o, where a is the legth of the Blumlein plate, and ν is the velocity of the electromagnetic wave in a material media.

For parallel plates the characteristic impedance (52,44,6) is:

$$Z_a = Z_b = \frac{377}{\sqrt{\epsilon_r}} \left[\frac{h}{h+W} \right] \ \Omega \qquad (2.3)$$

where **h** is the thickness of the dielectric medium, and included in the denominator as a correction factor for edge effects of the dielectric medium on either side of the Blumlein plate and should be constant in order to match the impedance of the storage and pulse forming lines.

The characteristic impedance of the laser cavity depends on the ionization level of the medium. For unpreionized parallel cylindrical electrodes with an electromagnetic wave propagating perpendicular to the electrode, the characteristic impedance Z_L has the same form as Z_a, with the electrode separation **d** substituted for **h**.

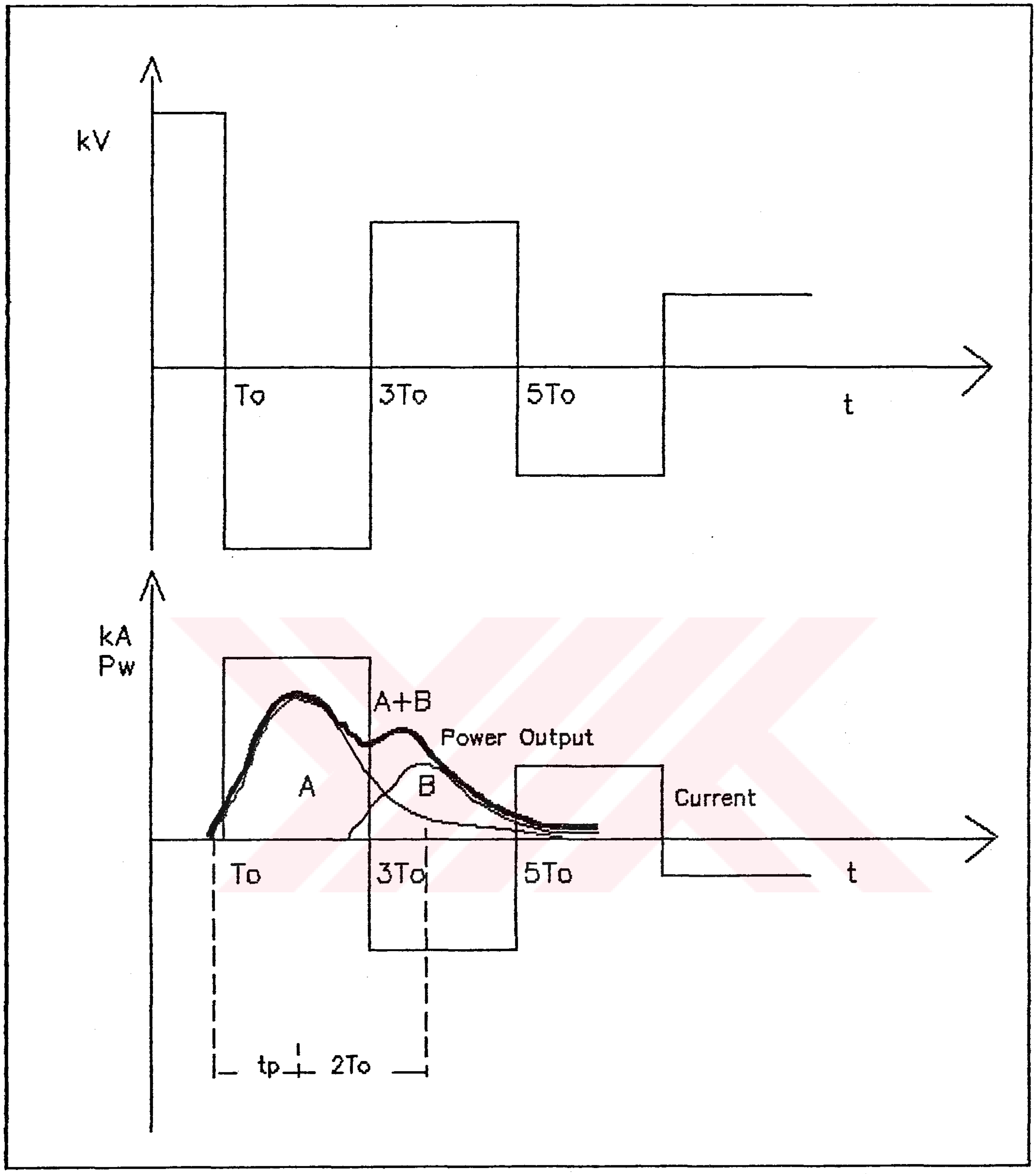

FIG 7: Multiple Reflections in the Blumlein-line between a Cavity of High Impedance and the Spark-gap (A is the forward and B is the reflected wave).

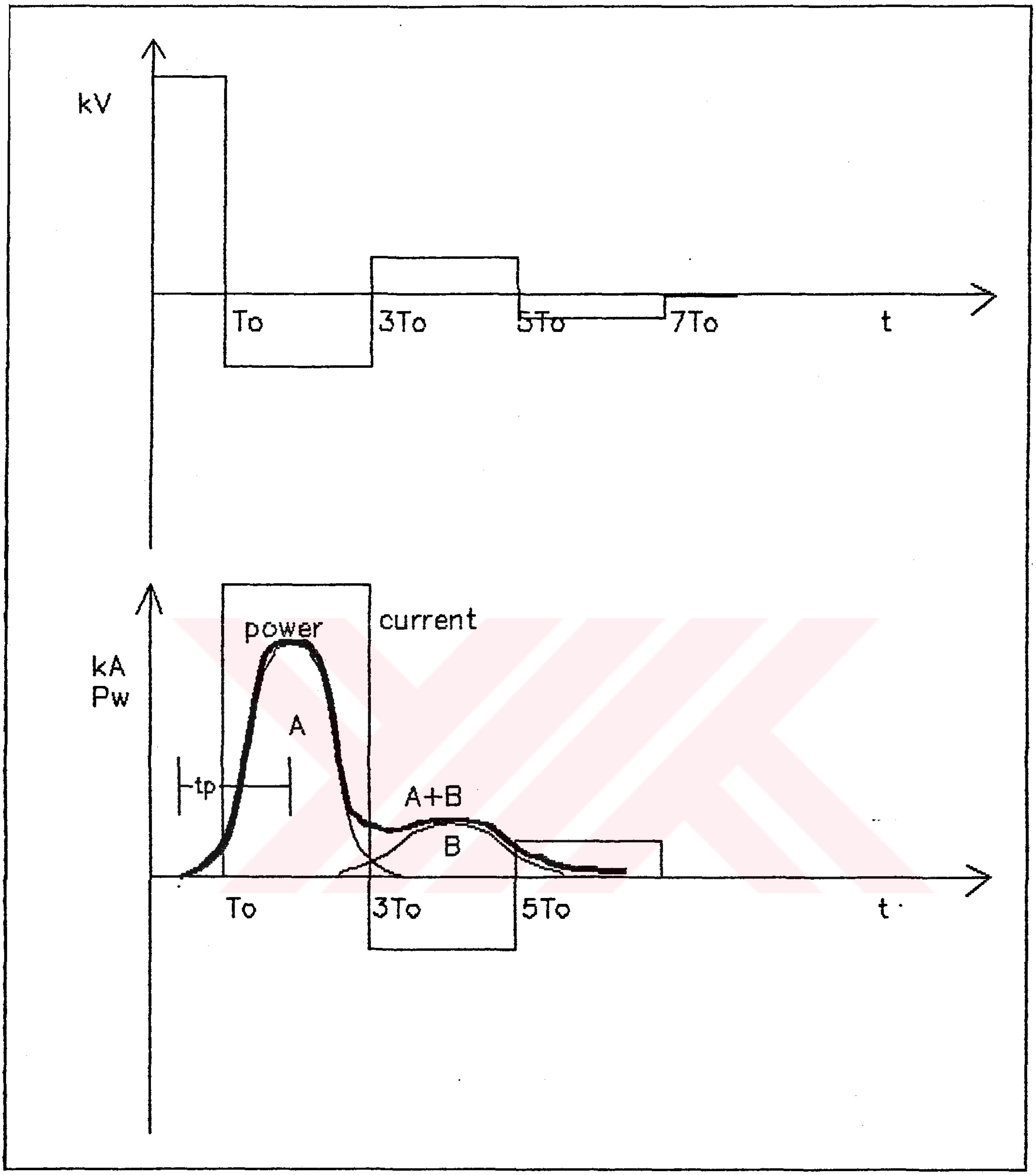

FIG 8: Multiple Reflections in the Blumlein–line with a low Cavity Impedance (intensity of the rear pulse is negligible compared with the front pulse)

In our system d=2.3 mm with capacitor width w=100 mm, we have Z_L=5.65Ω. This value is quite high compared to Z_a (1.5 Ω), and according to equations (2.1) and (2.2) most of the power is reflected, making it impractical for using the system in an unpreionized mode.

The characteristic impedance of the preionized system is nonlinear and depends strongly on the density of the gas and the discharge current, that is, to the extent that the gas has been ionized. The current-voltage relationship is given by **Marotta's** formula for high current discharge plasma,

$$V = \kappa I^{0.85} \tag{2.4}$$

where κ depends on plasma density (i.e. fill pressure).

The plasma discharge has the characteristic impedance:

$$Z_L = \frac{\Delta V}{\Delta I} = \kappa' I^{-0.15} \tag{2.5}$$

$$\alpha\, p^{-12/13}\ (d/r)\ I^{-0.15}$$

Where p is the gas pressure and r is the radius of the cylindrical electrodes.

The equation reveals that the impedance of the cavity is nearly inversely proportional to the fill pressure. At low pressures,the plasma impedance and reflected pulse amplitude are high, giving double pulses at the laser output. The effect can be shown graphically (figure 7 and 8). If the characteristic impedance of the plasma cavity is high because of the electrode separation or low gas pressure, multiple reflections between the spark gap and the cavity occur. The laser peak power would decrease and would be a superposition of two peaks resulting from the reflected and forward pulses. The duration between the two peaks, T_o, is then:

$$2T_0 = \frac{2a}{\nu} \quad , \qquad \nu = \frac{c}{\sqrt{\epsilon_r}} \tag{2.6}$$

When Z_L is reduced to the order of 0.1 Ω, it can be seen that the backreflected part is negligibly small and the peak power of the first pulse is enhanced.

Because of the high speed of the wave travelling through the dielectric, the **skin** effect becomes important. To minimize this effect the plates should be cleaned and if necessary polished. The skin effect, while reducing the output power, also delays the risetime of the step discharge pulse and broadens the pulsewidth. The time delay due to skin resistance along the transmission line is:

$$\tau_d = \frac{\rho \mu_0 a^2}{16\pi^2 Z_a h} \tag{2.7}$$

where ρ is the resistivity of the plate surfaces, and $\mu_0 = 4\pi \times 10\ \Omega s/m$ where Z_a is the characteristic impedance of the Blumlein plates. Variables a and h are the width of the Blumlein plate and the thickness of the dielectric between the capacitor plates,respectively (figure 6).

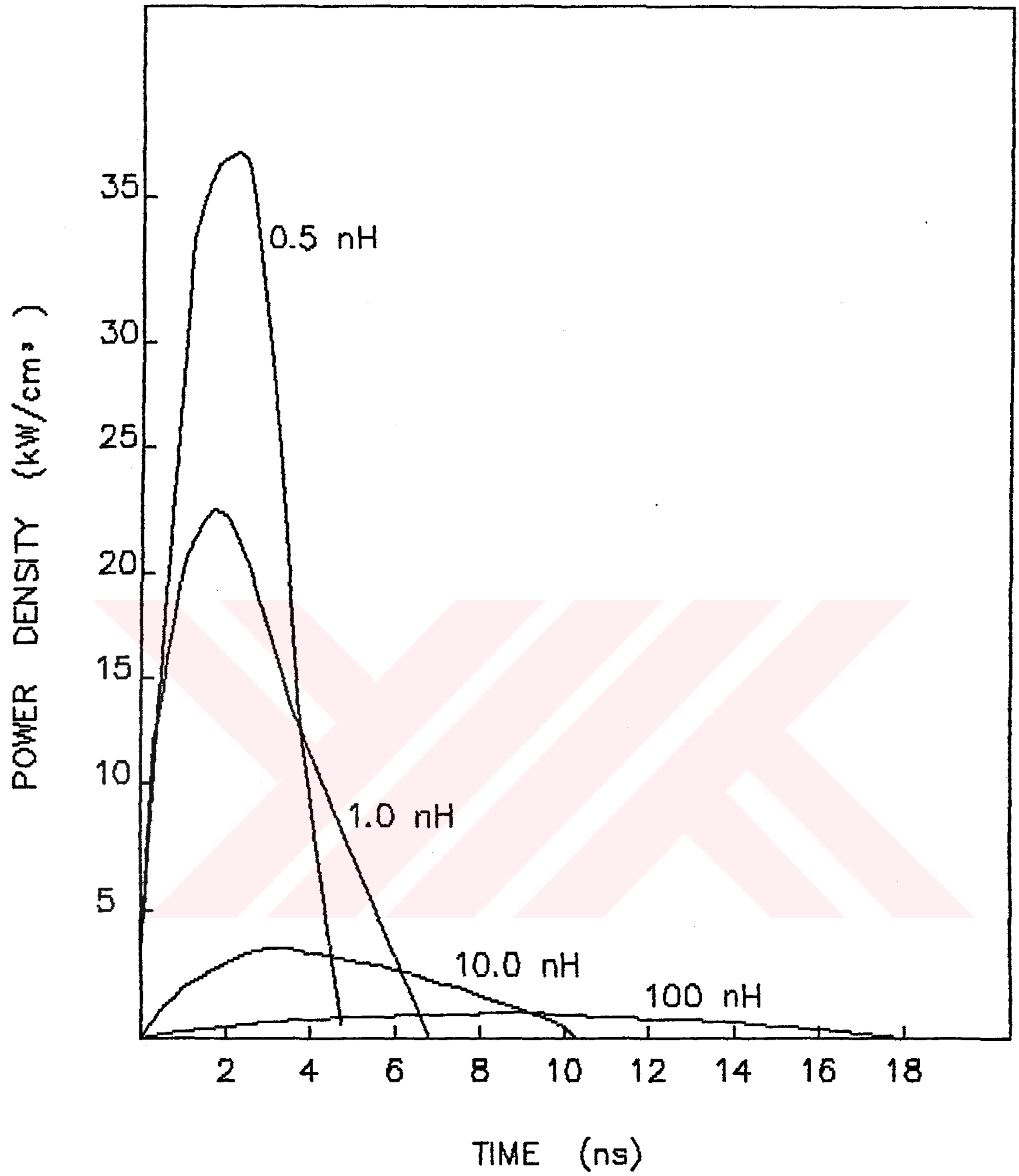

FIG 9: The POWER DENSITY as a FUNCTION of TIME for DIFFERENT CIRCUIT INDUCTANCES

2.3 Laser Power Density Calculations

The theory of the pulsed molecular nitrogen laser was described by **Ali** (12) and **Gerry** (13) where the nitrogen molecules are coupled to an electric field to form a laser oscillator. The electric circuit consists of an energy storing capacitor **C**, charged initially to some voltage **V**, a lumped circuit inductance **L**, a fixed resistance **R** (figure 4). The gas, as described previously acts as a varible resistance because of electron-molecule collisions. The upper and lower laser levels are populated directly from the ground state. The laser power density and related time history are calculated by solving numerically a system of coupled laser rate equations (28,29).

This section presents a qualitative overview of the solution of these equations.

The laser power density and its duration depend to a great extent on the current rise time as shown in figure 9. The laser

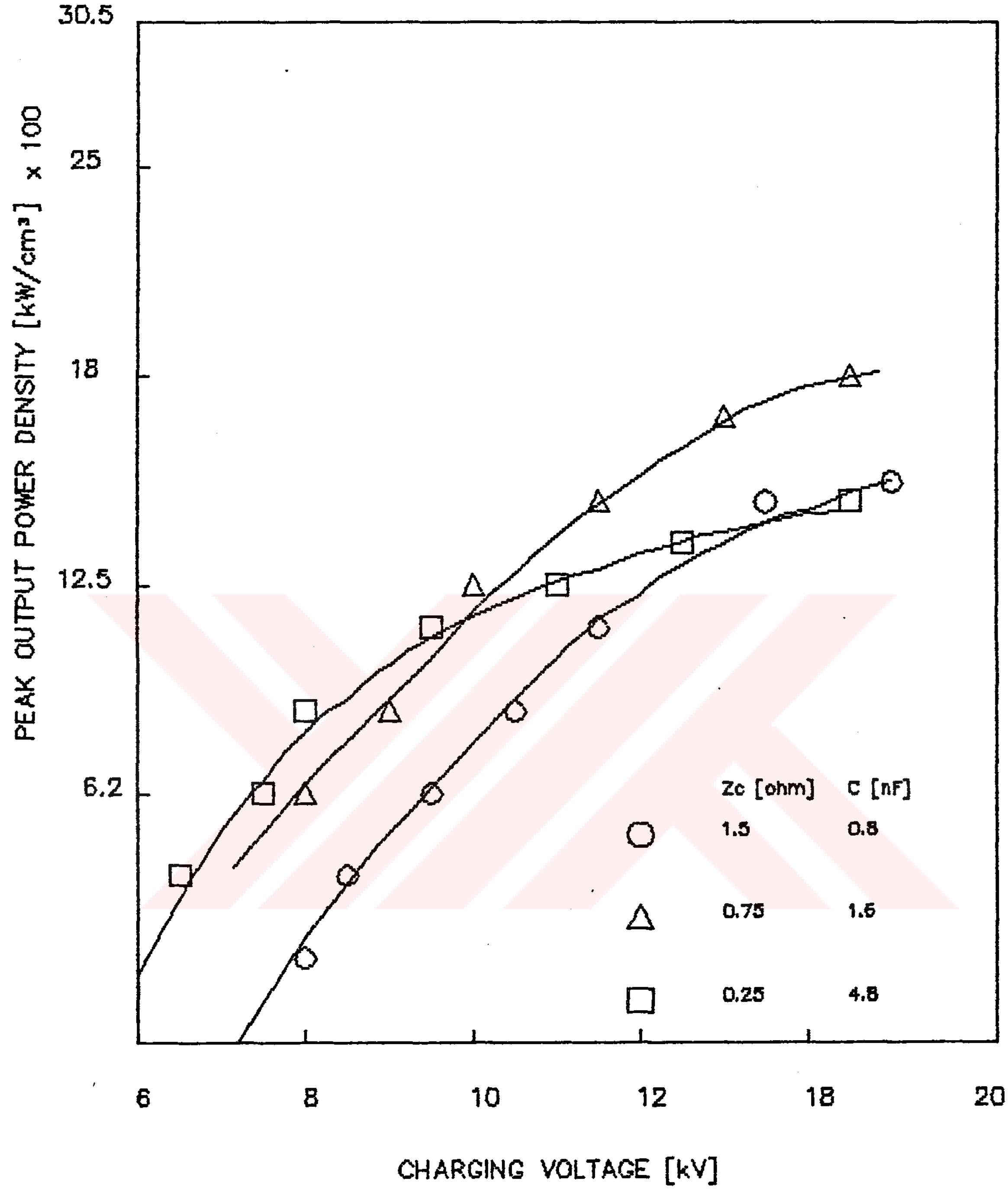

FIG 10: Effect of Blumlein Impedance
and
Charging Voltage on Peak Power
of a TEA N_2 Laser

power density and its time development are given for several values of circuit inductance. The total energy of the laser is larger for fast rising currents because both the ionization rate for high currents, with fast rise times and the electron temperature are higher than for low risetime current pulses. This is valid for the time period of interest. That is, the lifetime of the upper laser level. The lifetime of the C π_u laser level at a pressure p (in Torr) is given by (21)

$$\tau = \frac{36}{(1+p/58)} \text{ ns} \tag{2.8}$$

and is calculated to be 2.5 ns for atmospheric pressure.

The laser power density is proportional to the rate of the excitation of the upper laser level which is a function of the electron density and its temperature. The higher power densities result with increasing electron density and higher electron temperature. The hotter electrons lose less energy for the excitation of the ground state vibrational levels (12).

For electron temperatures below 6 eV, the rate of energy loss by electrons into the excitation of the ground state vibrational levels predominates over other rate processes,for example molecular ionization and the excitation of the upper laser level. The efficiency of N_2 laser system depends on having the electron temperature above 4 eV and thus reducing the energy loss by electrons by the excitation of the ground state vibrational levels.

The relationship for peak power density and the charging voltage for different capacitors are shown in figure 10 (20).

The laser power density is seen to increase with increasing voltage which can be attributed to intense electric field, leading to higher (electric field/pressure) E/p values. This results in higher electron densities producing higher currents and enables higher power (ohmic heating per unit volume) to be transferred to the gas system. The higher electron temperatures obtained results in more efficient excitation of laser levels producing higher peak power densities.

The narrowing of the power pulse remains to be explained. The laser line at 337.1 nm has a lower level which has a longer lifetime compared with the radiative lifetime, τ_c (44). This fact limits the derivation of the laser pulse t

to be less than τ_C, with higher laser power density, the induced emission rate predominates over the spontaneous decay. Since the effective lifetime is the inverse of the induced emission rate, smaller halfwidths are expected.

The mixing of the laser levels by electron impact and the electron impact ionization of the molecule from the C state would also influence the population density of the upper laser level, further shortening the duration of the laser pulse. Therefore the increasing electron density would lead to higher laser power density and eventually to narrower pulses.

2.4 Photopreionization of the Laser Cavity

The high pressure glow discharges can be produced in a variety of different gases by simultaneously initiating many overlapping electron avalanches in a homogenous electric field. The electrons can be obtained by volume photoionization and photocathode emission or can be extracted from a tenuous plasma formed between the electrodes. The electrons may thus be conveniently derived from the UV radiation or afterglow of a suitably priming discharge.

Since the 1970s when the glow discharge process was first used to excite laser systems (16,47), it has been extensively used in the double discharge excitation of large volume, high pressure lasers.

It was shown that the plasma can develop on nanosecond time scales (36). The fast formation of discharges was used to excite high pressure UV gas lasers and provided a physical basis for the development of fast, erosion-free low inductance, high voltage switches.

The application of the glow principle to UV N_2 lasers utilized the existing IR double-discharge technology to produce effective lasing action at high pressures (37).

Conventional laser systems with glow discharge plasma have shown that lasing is limited by the attainable excitation rate and discharge stability. The relatively high loop inductance tends to limit the excitation rate. The stability is strongly influenced by the intensity and distribution of the trigger discharge and by the timing between the trigger and main discharges.

The stabilization can be effected over a wide range of pressures and overvoltages. The principle is adapted to the nanosecond excitation of nitrogen lasers at pressures of up to five bars (17).

The glow discharge is formed by channeling current from a distributed (surface tracking corona-like) pilot discharge into the adjacent **"uniform field"** gap. The corona-to-glow switching process is affected automatically. The pilot and the main discharges are essentially derived from a single pair of appropriately contoured electrodes.

The simple arrangement shown in the figure 6 can be used to stabilize discharges over a limited range of elctrode spacings. The auxiliary corona electrodes serve to provide an initial (low energy) distributed corona discharge to photoionize and thus prepare the main gap for glow formation. The stabilization and glow uniformity can be optimized by adjusting the relative spacings between the blades and the main electrodes. The optimum blade separation is typically 20-40% greater than that of the main electrodes (49).The settings are reported not to be critical. Trace levels of a photoionizable additive, triethylamine were used to improve discharge uniformity at small electrode separations and high discharging voltages (45).The stability of the main glow discharge is relatively insensitive to the profile and surface quality of the main electrodes.

The discharge formation and stabilization processes derive from a combination of electron seeding and compensated inductive switching effects; the details are not well understood. Qualitatively it can be expained as follows. The corona serves to photoionize the main gap and condition it for a glow formation. A corona-to-glow transfer becomes favorable when the gap resistance is low enough for inductive effects to become dominant. The corona discharge can have a significantly higher effective inductance than the main glow discharge. The effective expansion of the plasma can then compensate for the apparent increase in inductance in current by lifting the discharge into the main uniform region.

The qualitative explanation is supported by the fact that the glow discharge is confined only to discharge regions that are photoionized. In order to have a uniform glow, a well distributed corona discharge is necessary. The experiments clearly showed that the reason for stabilized glow discharge is an effect of corona discharge (47).

III . EXPERIMENTAL SYSTEM

3.1 Electronic Circuitry

The electronic circuitry of the nitrogen laser is a simple DC-to-DC converter without any consideration to power requirements or current rating.The built-in unit can supply DC voltages up to 40KV and sufficient current to sustain a two hertz pulse rate. For higher repetition rates or more controlled pulse shapes, it is necessary to use a separate HV power supply with the appropriate specifications.

The full circuitry is given in figure 11. The line voltage is rectified and filtered via **R1, Z1** and **C1** to obtain a low voltage DC level. Through **D1** and R2 transistor **T1** is made to cut triggering at positive half cycles which enables **D2** to charge **C2** rapidly, without resistive power dissipation. **R3** connected to the collector of **T1**

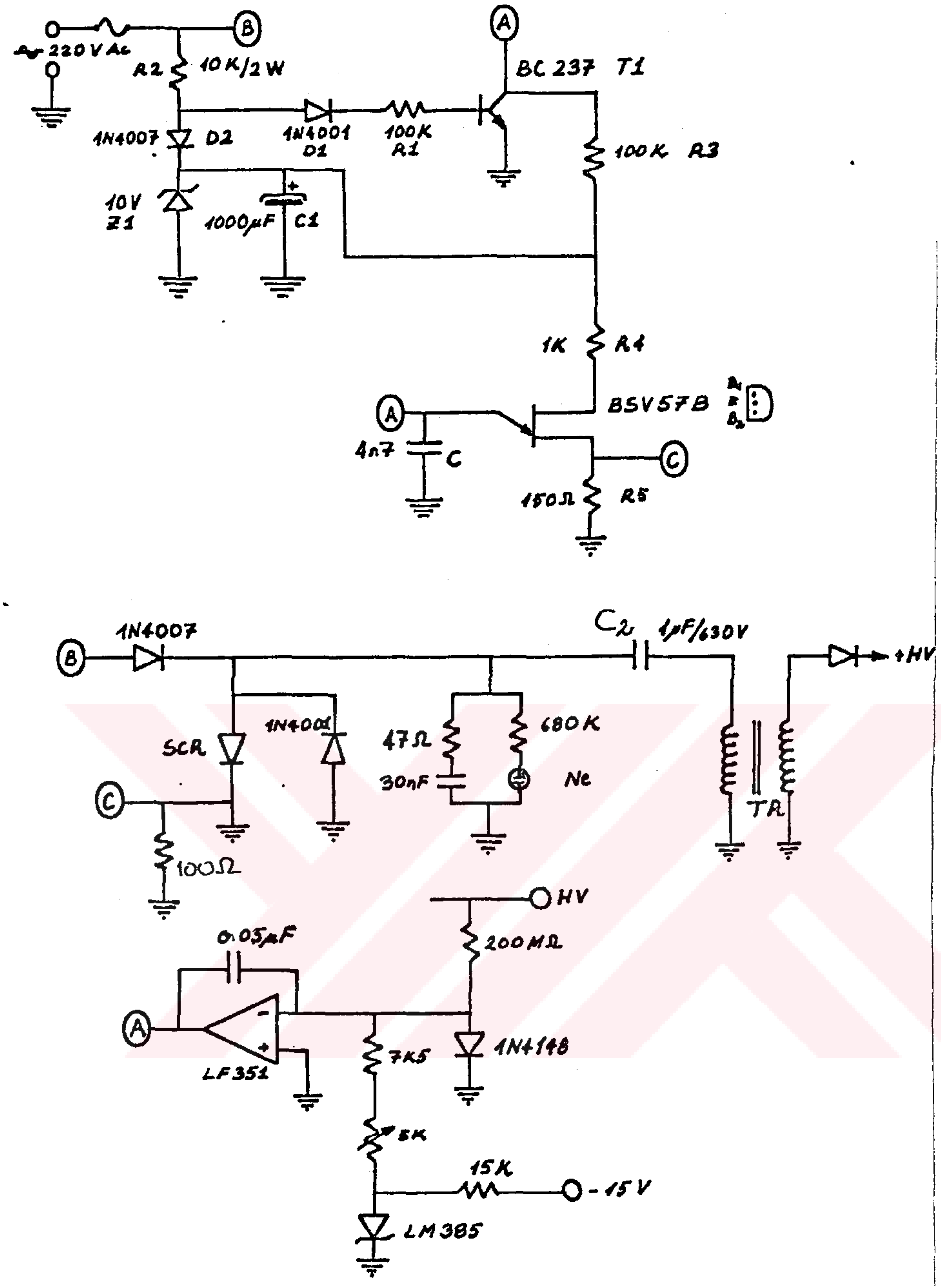

FIG 11 : LASER POWER SUPPLY

charges **C** which determines the frequency of oscillation and triggering pulse. The capacitor value, **C** is critical at two points :

i. It sets the oscillation frequency,
ii. It supplies the gate current.

Therefore it should be noted that, for low **SCR** voltages (<40 V) higher values of **C** should be used and vice versa. Since **T1** controls the rate of oscillation, it may also be used for **HV** regulation (see the schematic for regulation add-on).

However, since the voltage level is determined by the spark gap, there is no need for **HV** regulation in the free-running mode.

3.2 Mechanical Construction

The compact construction of the laser allows it to be extremely portable but restricts the ability to adjust and measure some of the experimental constraints.

The whole unit is machined from plexiglass material (figure 12b). The plexiglass box need not necessarily be gas-tight, but for a homogenous gas flow and economic gas usage it is preferable. The main block is used to hold the laser cavity block, inductor, spark gap and transmission line (figure 12e).

The bottom of the block has a recess to contain lower half of the spark gap assembly. An O-ring ensures that the complete spark gap is gas-tight when compressed against the capacitor plates. Electrical contact with the capacitor is also made by compression. The block has a separate gas inlet for cooling the spark gap assembly and the removal of any particles that form during the arcing process.

The plasma cavity is another removable unit and comprises the cavity mirror holders and electrodes. The aluminium electrodes are machined in such a shape that the plasma should form only in the center of the gap (figure12c, 12d).

The surface finish and exact alignment of the electrodes do not greatly affect the lasing action (48,47,22). Therefore the electrodes are only roughly ground and then polished.

At each end of the cavity a mirror is mounted in a perspex holder. The holder can be adjusted by three spring loaded screws equidistantly spaced around the edge of the holder and mounted directly on the plasma cavity block (figure 12 f).

The unit allows the gas to flow out from two ports, one in the spark gap assembly and the other in the cavity volume. The second port also doubles for the output window which is left open, to maximize UV transmission. There is enough space for the electronics inside the box, but connections are provided to allow the use of external power supplies if required.

The capacitor plate, which acts as a transmission line, is made from polyethelene sheet obtained by bleaching an X-ray film, and covered with thick aluminium foil. It was seen that use of soft metal foils is better to overcome sparking from sharp edges and unexpected parts. The aluminium foil was glued to the polyethelene dielectric sheet with a special adhesive, **Polip Kleber 311.** Double sided adhesive tape can also be used. However this usually results in a lower value, nonlinear

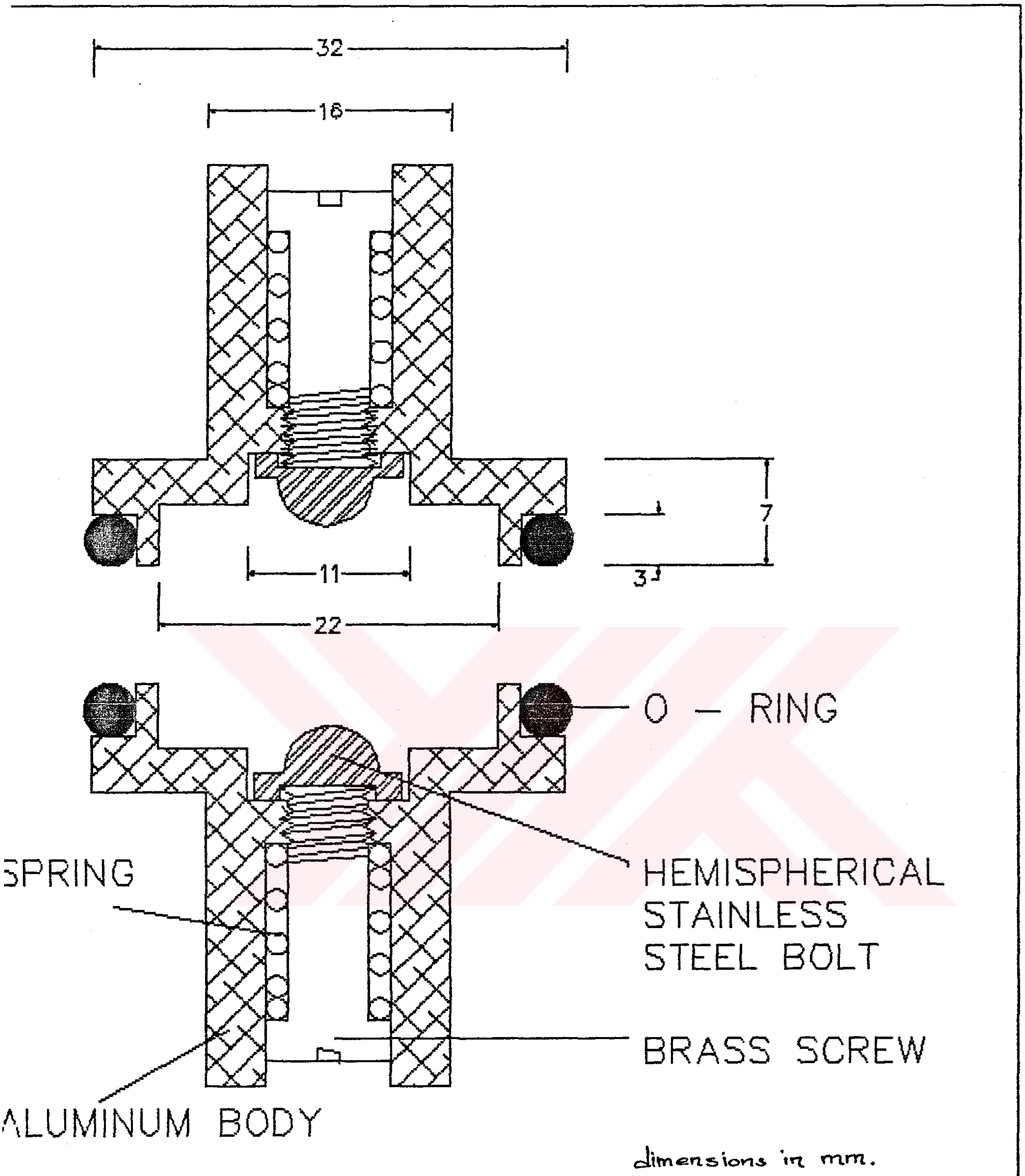

FIG 12a: SPARK GAP CONSTRUCTION

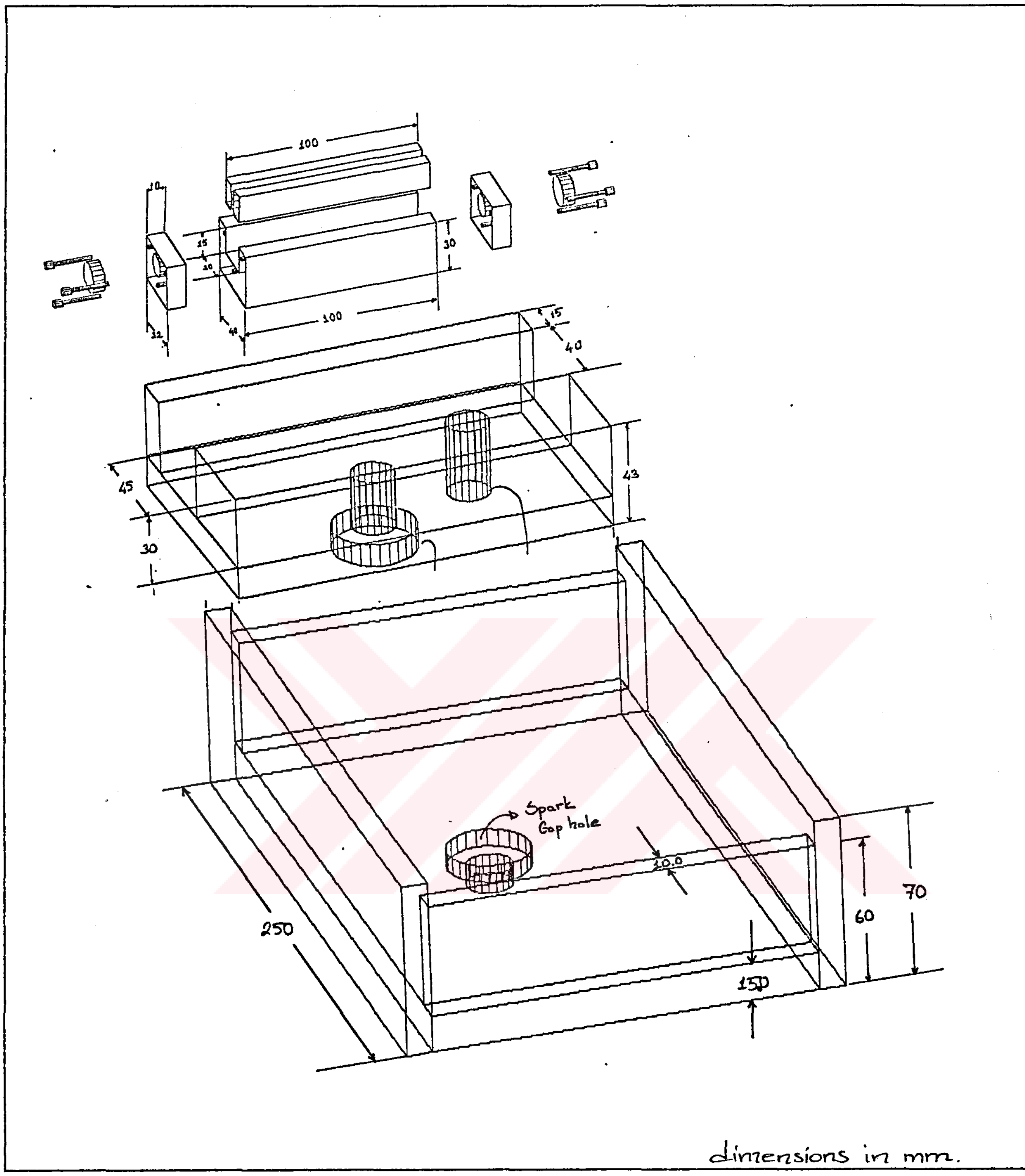

FIG 12b:

NITROGEN LASER
MECHANICAL STRUCTURE

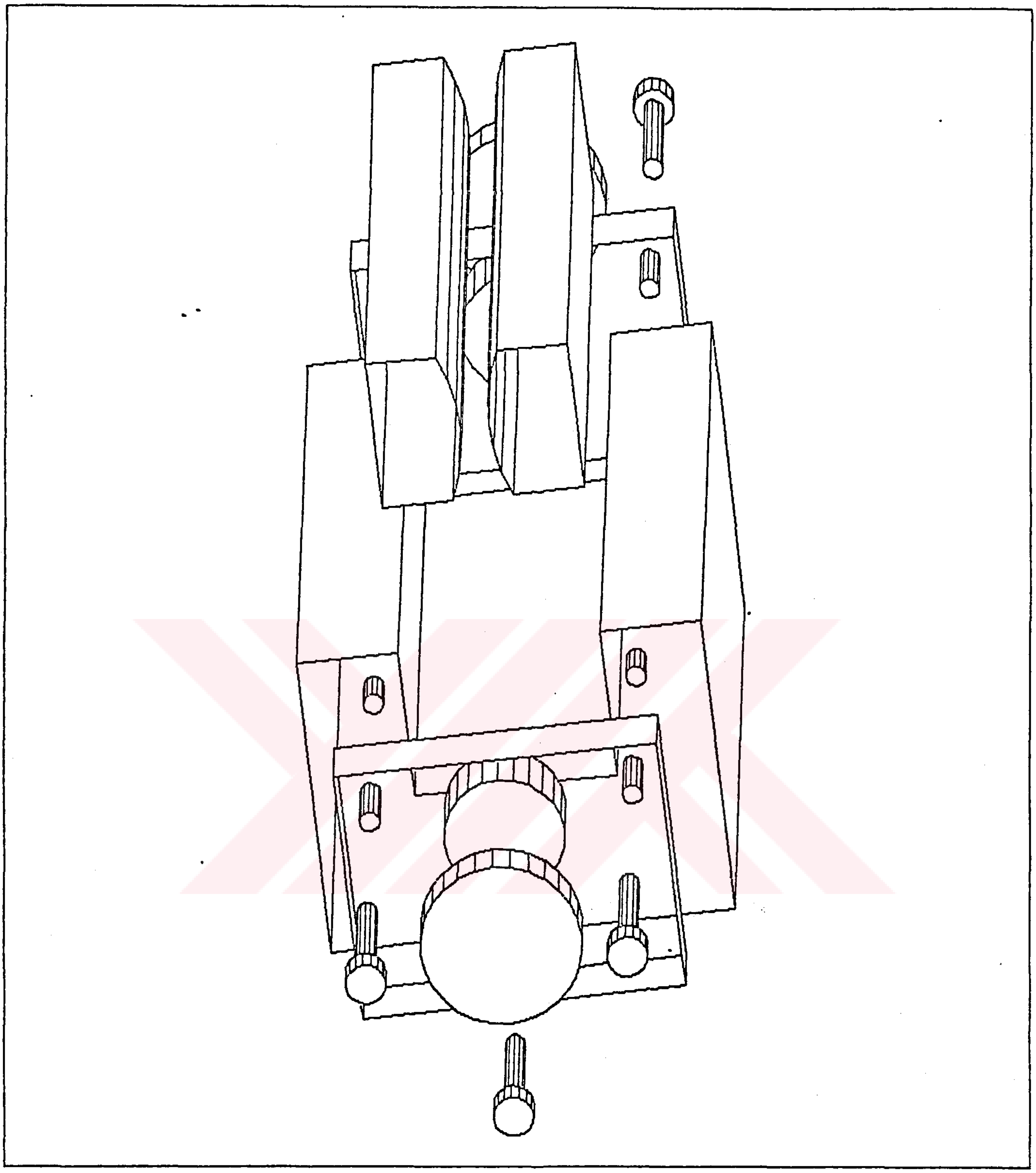

FIG 12c:

NITROGEN LASER
PLASMA CHAMBER STRUCTURE

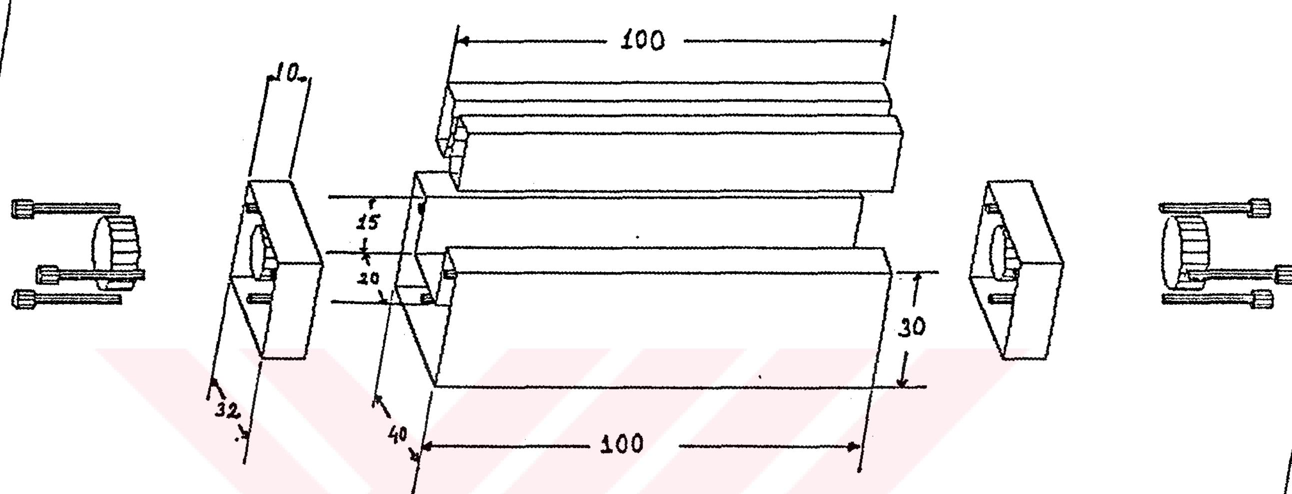

FIG 12d:

NITROGEN LASER
PLASMA CHAMBER STRUCTURE

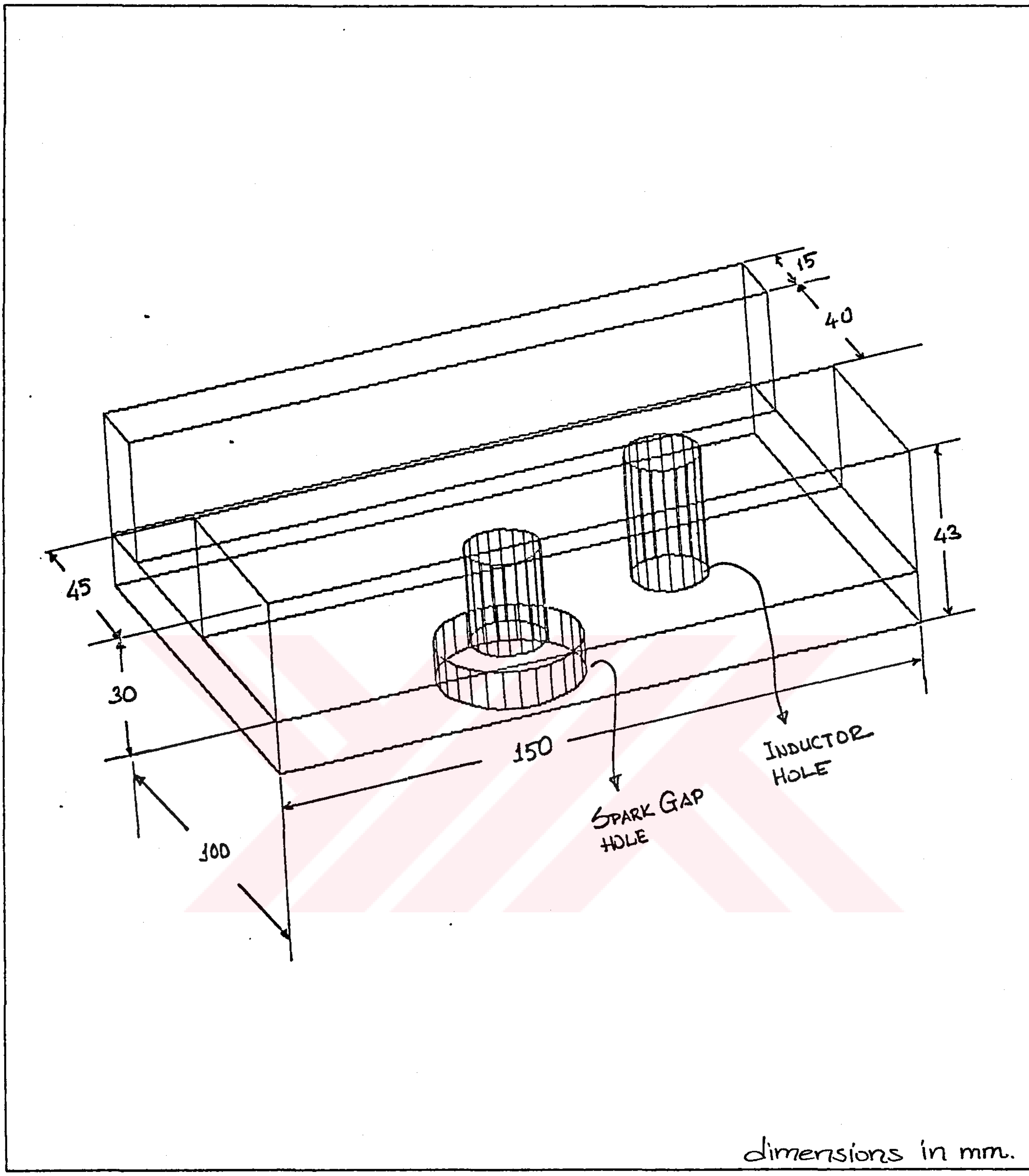

FIG 12e:

NITROGEN LASER
MAIN BLOCK STRUCTURE

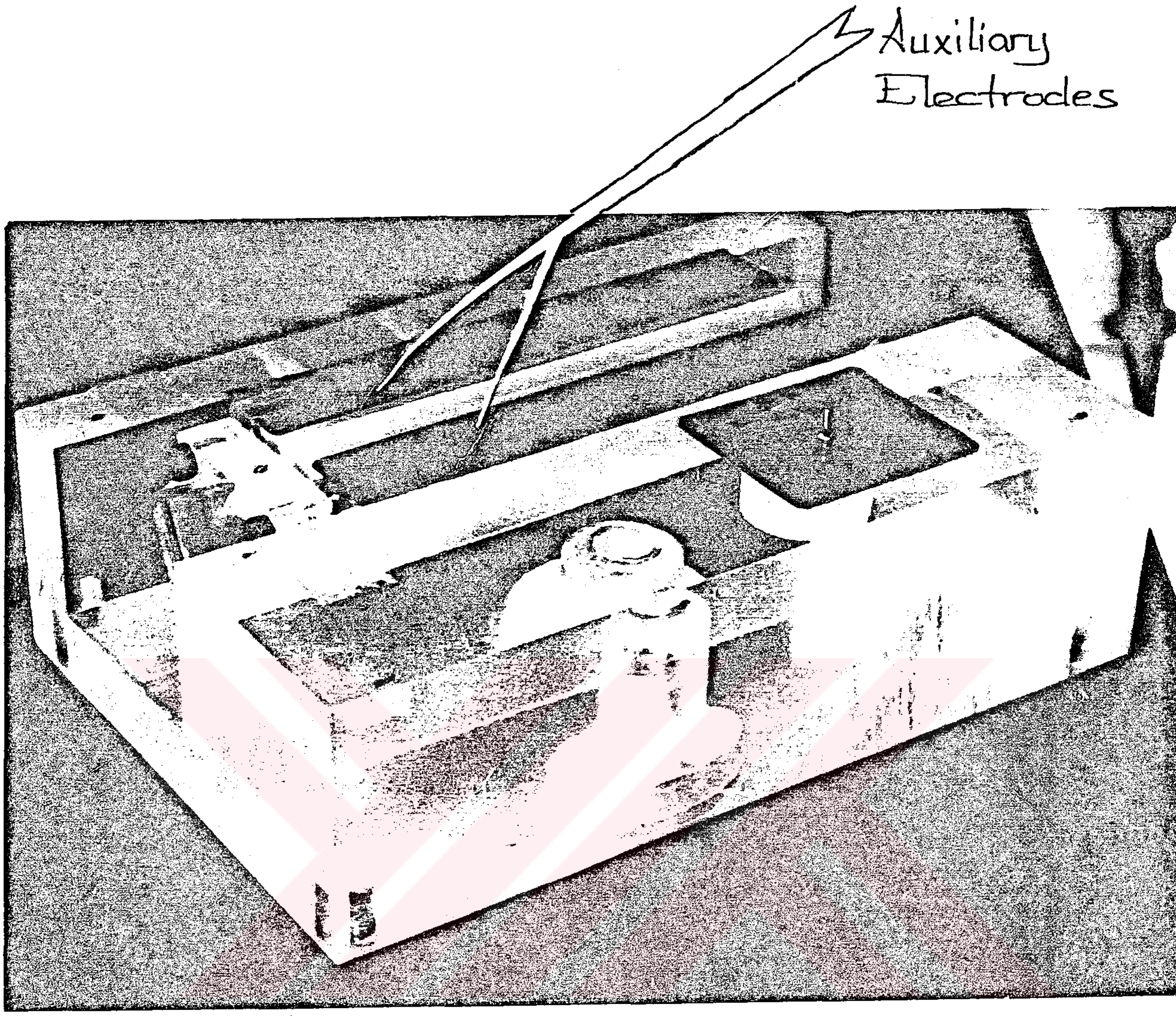

FIG 12e:

NITROGEN LASER
MAIN BLOCK STRUCTURE

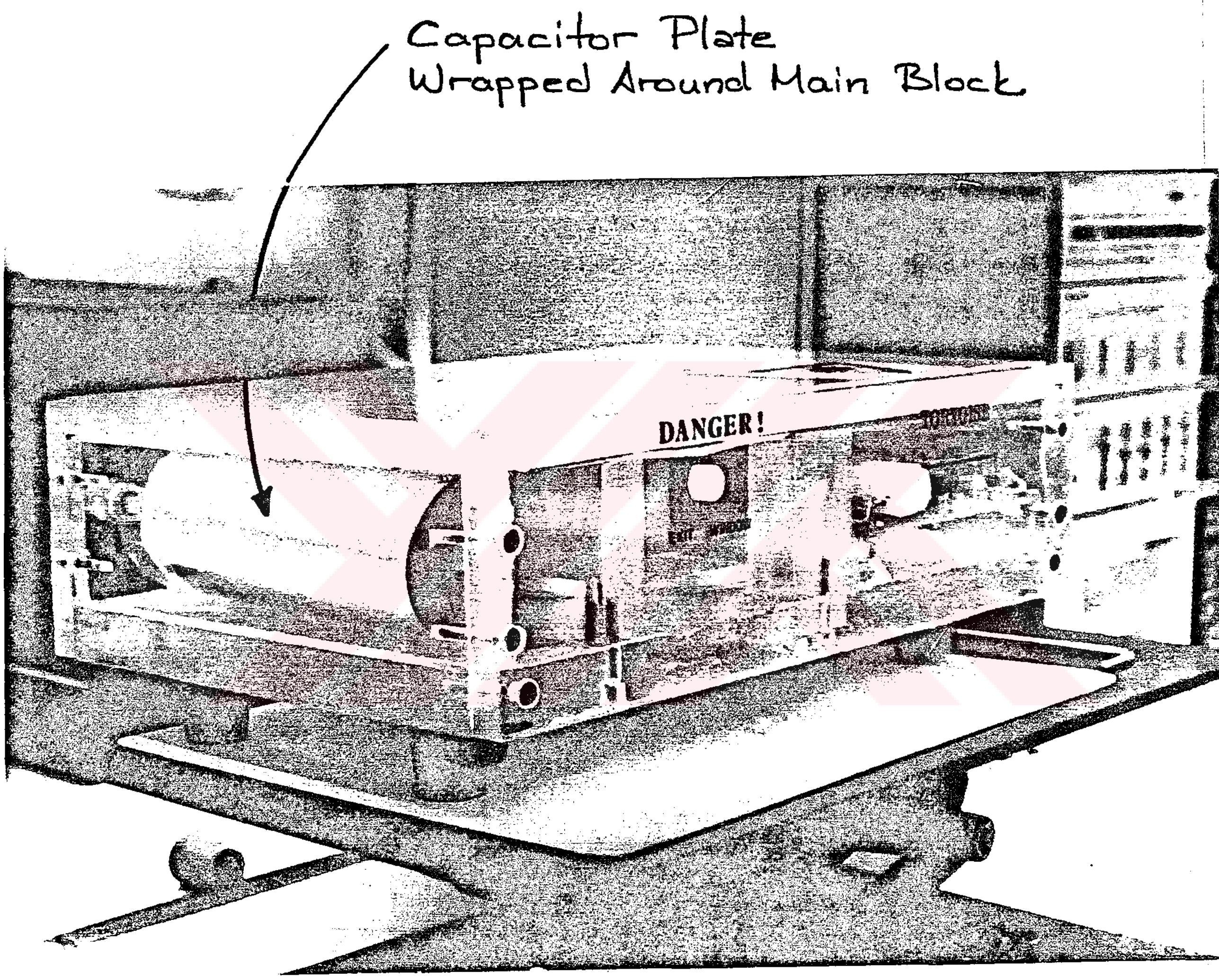

FIG 12g:

NITROGEN LASER

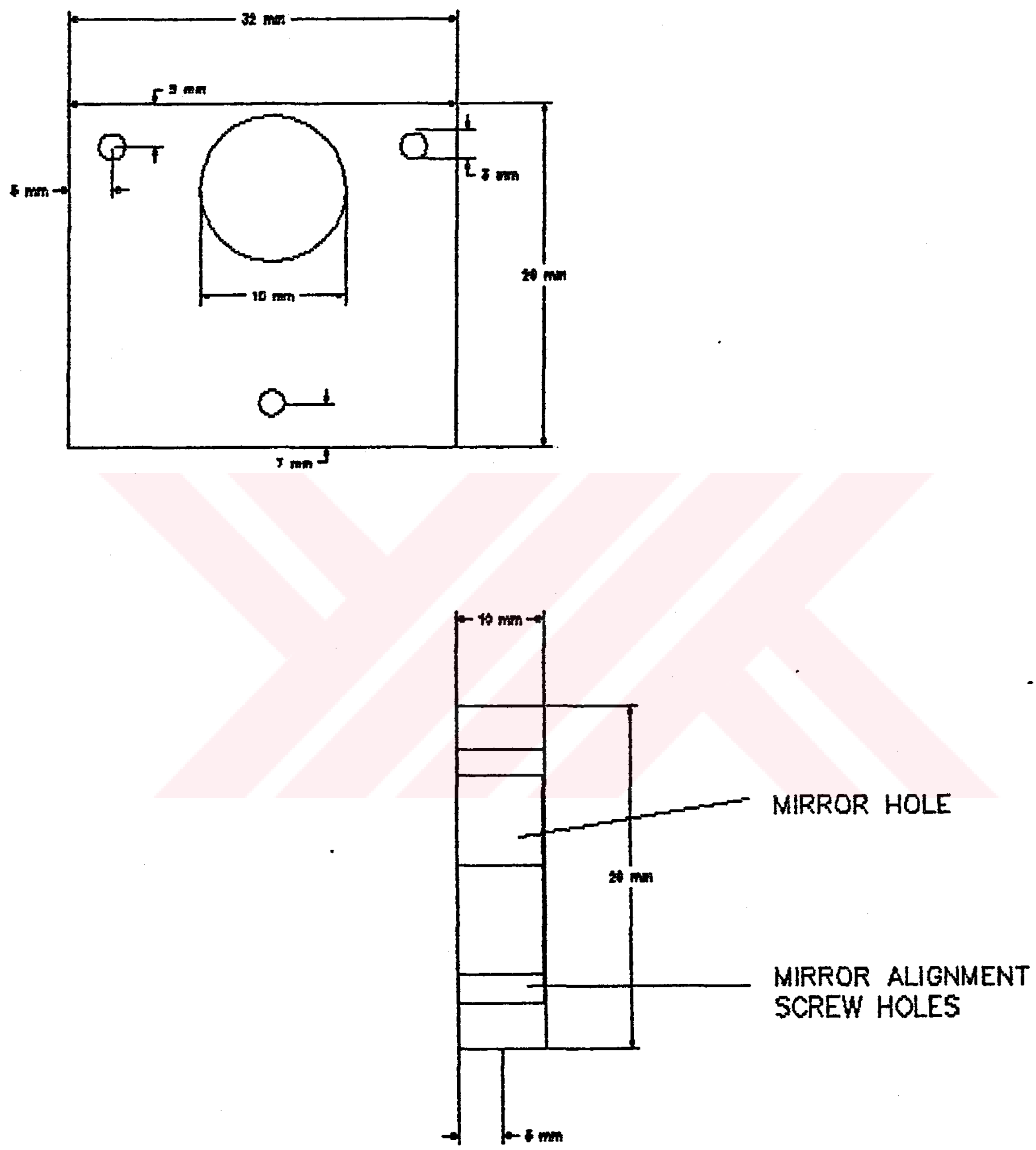

FIG 12:f:

MIRROR HOLDERS

capacitor causing uneven triggering and hence an unstable laser output.

The electrical connections to the Blumlein plates and electrodes are all made with pressure contacts. Therefore care should be taken for the cleanliness of the contact points and surfaces. The nitrogen gas enters from two different hoses into the system: one input connects to the laser cavity whilst the other connects to the other. This gas flow configuration easily and quickly fills the discharge volumes, with no ozone or other free radical production which would also destroy the electrode surface finish. In this configuration, the spark gap can be pressurized to give higher breakdown voltages.

The spark gap is machined from aluminium. Hemispherical stainless steel bolts are used as electrodes. One end of the spark gap is accesible through a hole in the bottom of the box. This permits easy adjustment of the spark gap (figure 12a).

Units are connected to each other with allen bolts to enable easy component replacement and necessary places are covered with silicone rubber for gas-tightness.

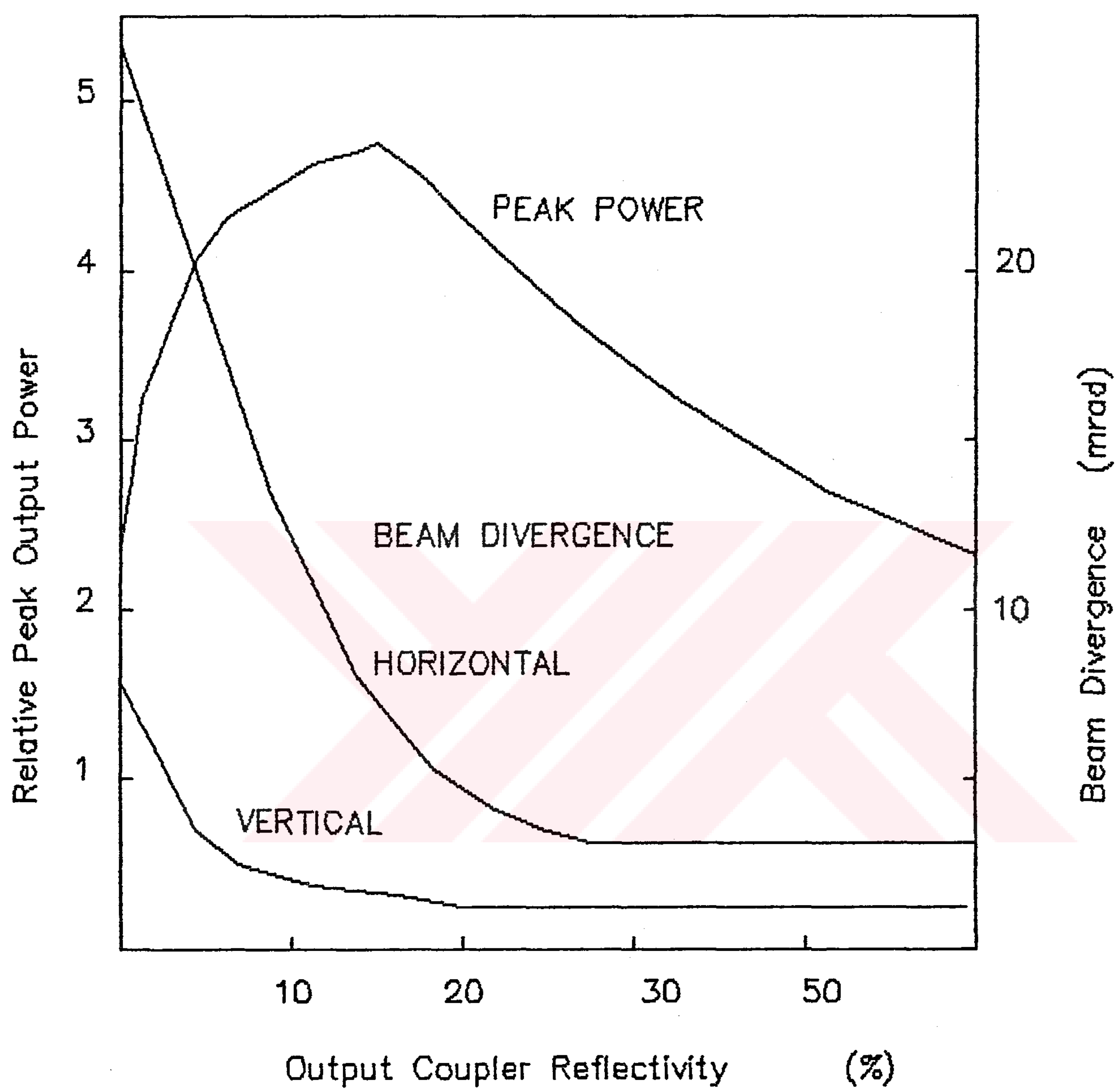

FIG 13: PEAK OUTPUT POWER and BEAM DIVERGENCE

3.3 Optical System

The optical system of the laser is very simple because of the short pulse duration is comparable to the lifetime of the upper laser level. Since the laser is working in the bidirectional mode, an end reflector is included. First a dielectric coated UV mirror was used but because of the problems with the quality of its surface an aluminium coated reflector was substituted. It has a reflectivity of 92 per cent and an increase of output power with a factor of two to three is reported elsewhere (22,21,53,54). **Hasson** et.al. (22) reported that the inclusion of the output coupler with reflectivity of 12-18 per cent would not only increase the output power but also decrease the beam divergence substantionally which can be compared in the figure 13.

The output window can be made of quartz microscope slides, however we prefered it to be left open to be used as a gas outlet.

The beam divergence is a function of the discharge region length and width, which results with an elliptically shaped beam. For our cavity:

$$\begin{aligned}\theta &= \frac{d}{L} \text{ rad} \\ &\approx \frac{2.3}{100} \approx 20 \text{ mrad}\end{aligned} \qquad (3.1)$$

However when the back reflector is used, the effective length is doubled with a horizontal divergence of ≈10 mrad. The vertical divergence is function of vertical length of plasma formation region which is usually quite small. The coherency of these systems is quite low, with a value of ≈27mm measured using a michelson interferometer with a laser cavity of 270 mm length (23).

3.4 Measurement of Optical Pulses

Concerned with the measurement of optical pulses from a nitrogen laser with wavelength of 337.1 nm and nanosecond regime there are several problems among which an important one is the spectral region of detection, and another is detection of high speed pulses.

A design of high speed photodiode assembly is given by Mc Call, with 100 ps risetime (55). A sampling oscilloscope is used to detect the pulses.

Another inexpensive method for pulse-width measurement is to use the reverse biased emitter to base junction of an open microwave transistor (HP 35832 E) (19). This transistor's epitaxial layout leaves some of the base region exposed, permitting photoexcitation . A simple calculation for photodiode and scope combination measurement system can be done as follows:

Because of the finite system-response time, the actual pulsewidth should be different and necessarily be smaller than that of the observed pulse. If the observed pulsewidth is

t_{obs}, and the rise-time of the oscilloscope is t_{sc}, the photodiode source resistance is R_g and scope input resistance R_{in} with a shunt capacitance C_{in}, we have an input charge time; t_{inp}, with equivalent charging resistor R_{ch}:

$$t_{inp} = 2.2\, R_{ch} C_{in}$$

$$R_{ch} = \frac{R_g\, R_{in}}{R_g + R_{in}} \qquad (3.2)$$

then the laser pulse duration t_g can be estimated to be (44):

$$t_g = \sqrt{(t_{obs}^2 - (t_{sc}^2 + t_{inp}^2))} \qquad (3.3)$$

In order to measure the laser output energy the photodiode energy can be calibrated with a laser of known characteristics, such as a GaAs laser (25,56,57,58).

To find long term performance or energy distribution of the nitrogen laser, a multichannel analyzer can be used (59).Streak cameras are also used for fast optical pulse measurements (24) where the time resolution is on the order of 10 ps.

3.5 N_2 Laser Pumped Dye Laser System

The nitrogen laser was designed for pumping a dye laser. The dye laser was designed to work on an optical breadboard. The dye solution is in an HV transparent optical quality cuvette which lets 337.1 nm nitrogen laser radiation to pass through. Referring to the previous studies, we have first tried to observe superradiant emission from **Rhodamine 640** solution and **Disodium fluorescein** solution.

For a high optical quality dye laser beam with a small band-width and stability as well as higher coherence; we have planned to use the dye solution in a **Fabry- Perot** cavity with the backreflector replaced with a diffraction grating which allows fine tuning of the wavelength of the output beam. The diffraction grating is planned to be coupled to a

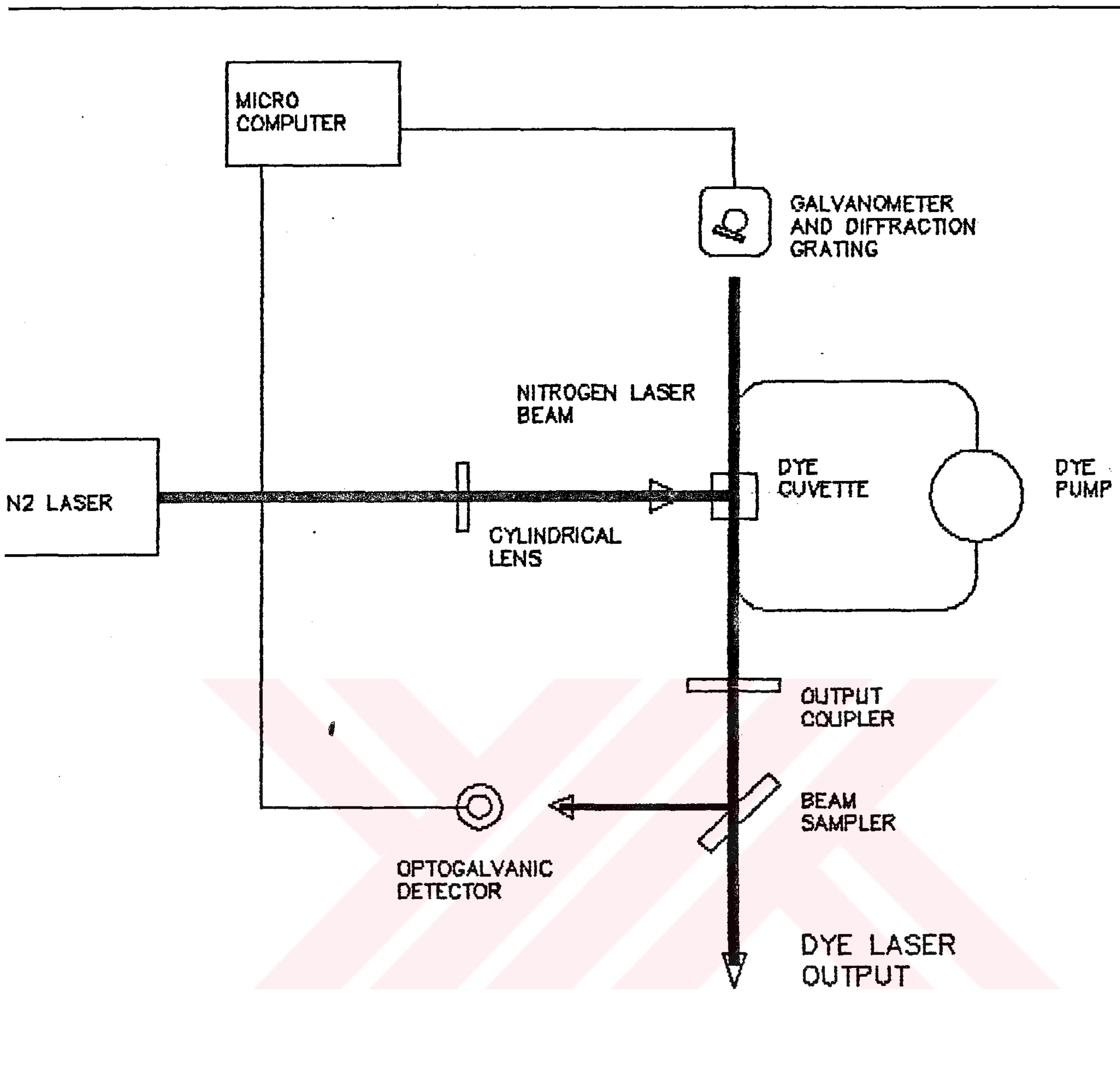

FIG 14: NITROGEN LASER PUMPED DYE LASER SCHEMATIC DIAGRAM

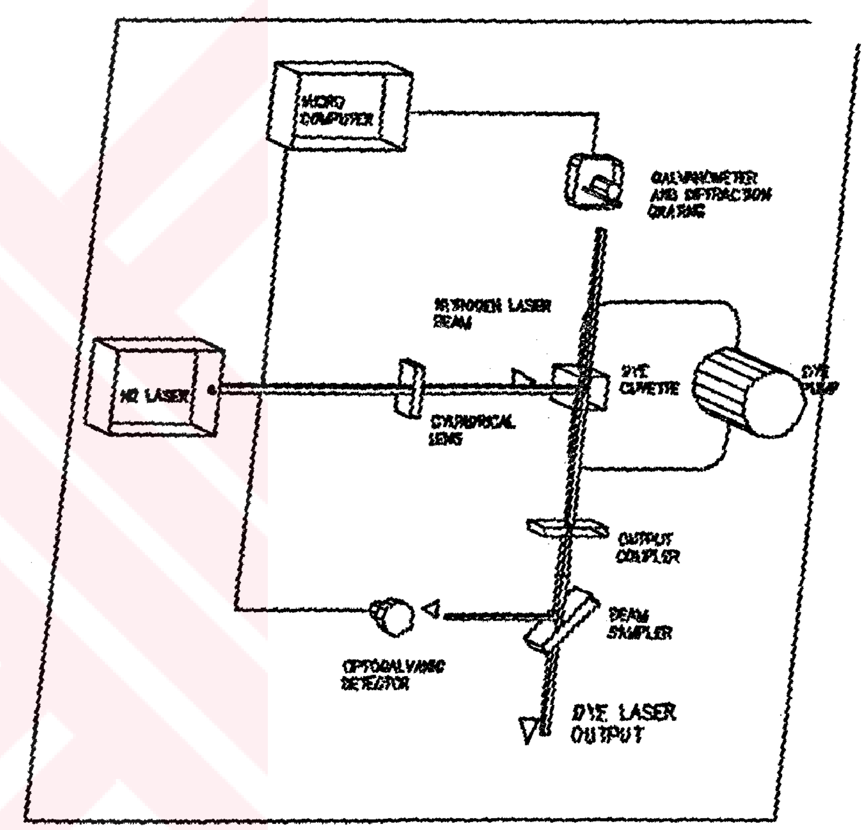

FIG 14: NITROGEN LASER PUMPED
DYE LASER
SCHEMATIC DIAGRAM

galvanometer which enables electronically controlled tuning. The galvanometer is a part of a digital control system under the supervision of a personal computer used for data collection, control and analysis. The accurate wavelength tuning could be achieved with a real time spectroscopic analysis done with the **optogalvanic** effect which is the change of plasma resistivity upon illumination with light and as a function of wavelength. Then the measured wavelength of the output pulses would be used to control the diffraction grating via the computer, thereby the output wavelength (figure 14).

The dye laser setup has not been completed in the way it is designed yet. However experiments related to fluorescence and superradiant effects are being conducted.

3.6 Qualitative Observations on the N_2 Laser Beam

The observed beam pattern from the nitrogen laser with the output coupler removed, that is, with an effective cavity length of 20.0 cm, is an ellipse, filling a rectangular area of 6cmx4cm at a screen 5m away from the laser. The beam divergence is roughly equal to the value calculated via eq.3.1, on the horizontal axis. The vertical beam divergence is a function of the plasma distribution inside the cavity, for which the theoretical calculations do not exist.

With the output coupling mirror removed the beam is very homogeneous, with a lower intensity, and greater divergence. The misalignment of the back-reflecting mirror gave rise to non-homogenous intensity distributions because, the decreasing divergence as a result of stimulated emission caused by the back-reflected photons only occured on a part of the beam pattern.

The output coupling mirror has the effect of increasing beam intensity and decreasing the divergence. However the misalignment of the cavity results with a highly irregular intensity distribution, which would be quite problematic in pumping the dye laser.

CONCLUSIONS

This work, which was planned to be a part of the microcomputer controlled dye laser system for solid-state and quantum-optics studies is the design, construction of the transversely excited atmospheric (TEA) molecular nitrogen laser.

Lack of necessary hardware (optical and electronical) slowed down our studies to a great extent. However, the nitrogen laser described before is working properly and can supply useful pulses of energy (qualitatively). Our continuing plan is as follows :

The rigorous theoretical analysis of TEA nitrogen lasers in order to find pulse lengths, coherency and optical power output. This is because of insufficient information and theoretical work on the atmospheric pressure very high gain lasers. Also the study of the superfluorescent emission will hopefully clear the problem of the way to describe these laser systems.

Completition of the dye laser system, which will be wavelength tunable via a personal computer driven diffraction grating used as a backreflector and spectroscopic analysis done with optogaluamic effect fed into the computer to fine control the output beam.

Use of the nitrogen laser in shadowgraphy to measure parameters of the shock wave created by a HV capacitor discharge.

Photoconductivity measurements in semiconductors with fast UV- nitrogen laser pulses.

It was realized that for experimental purposes, one does not need compact devices which bring complexities to align or optimise the laser parameters. Therefore it should be better, easier and more pleasant to design the laser with elementary geometries such as planar Blumline plates, cylindrical discharge electrodes, etc. Then it is quite easy to make the electrodes, mirrors and the spark gap adjustable even in operation. However it has the disadvantage of covering a large area and the risk of a mechanical failure.

It is hoped that this theses will give a better insight and pave the way for the development of techniques which will provide a useful tool for the analysis of various physical phenomenon via excitation with fast powerful pulses.

REFERENCE LIST

[1]H.G.Heard,Nature V200, 667 (1963)

[2]E.T.Gerry, Applied Physics Letters V7, 4 (1965)

[3]D.A.Leonard,Applied Physics Letters V7, 4 (1965

[4]J.D.Shipman, IEEE J Quantum Electronics QE2, 298 (1966)

[5]M.Geller, D.E.Altman, T.A. De Temple, J Applied Physics V39, 3639 (1966)

[6]M.Geller,D.E.Altman, T.A. De Temple,Applied Optics V7, 2232 (1968)

[7]J.H.Crouch, W.S.Risk, The Review of Scientific Instruments V43, 632 (1972)

[8]J.G.Small, R.Ashari, The Review of Scientific Instruments V43, 1205 (1972)

[9]J.Walker, Light, Freeman, (1982)

[10]Fruhgel, High Speed Pulse Technology V2, Academic Press (1968)

[11]A.W.Ali, A.C.Kolb, A.D.Anderson, Applied Optics V6, 2115 (1967)

[12]A.W.Ali, Applied Optics V8, 993 (1969)

[13]E.T.Gerry, Applied Physics Letters V7, 6 (1965)

[14]D.A.Leonard, **Applied Physics Letters V7,** 4 (1965)

[15]V.Hasson, H.M.von Bergmann, **J Physics E V9,** 76 (1976)

[16]A.K.Laflamme, **The Review of Scientific Instruments V41,** 1578 (1970)

[17]J.Koppitz, **J Physics D,** V6, 1494 (1973)

[18]A.Suedberg, L.Hogberg, and R.Nilson, **Applied Physics Letters V12,** 102 (1968)

[19]E.E.Bergmann, N.Eberhardt, IEEE **J Quantum Electronics QE9,**853 (1973)

[20]V.Hasson, H.M.von Bergmann, **The Review of Scientific Ins V50,** 59 (1979)

[21]B.S.Patel, **The Review of Scientific Ins V49,** 1361 (1978)

[22]H.M.von Bergmann, A.J.Penderis, jpe V10, 602 (1977)

[23]W.Herden, pl V54A, 96 (1975)

[24]R.Necafzadeh, Ph.D. Thesis, Lehigh University (1985)

[25]E.E.Bergmann, **Applied Physics Letters V28,** 84 (1976)

[26]H.Strohwald, H.Salzmann, **Applied Physics Letters V28,** 2721 (1976)

[27]P.Sorokin, **Lasers and Light,** Freeman (1972)

[28]J.A.Myer, C.L.Johnson, E.Kierstead, R.D.Sharma, I.Itzken, **Applied Physics Letters V16,** 3 (1970)

[29]B.Yan, **Chinese Physics V1,** 439 (1981)

[30]L.W.Braverman, **Applied Physics Letters V27,** 602 (1975)

[31] see refs.11 and 13

[32] see ref.12

[33]R.H.Dicke, **Physical Review V93,** 99 (1954)

[34]R.H.Dicke, **Lasers,** ed.J.Weber, Gordon and Breach, 29 (1968)

[35]R.H.Dicke, **U.S. Patent Office,** 2,851,652 pat.Sep 9,1958

[36]W.Mallory, pra V11, 2036 (1975)

[37]F.A.Hopf, pra V20, 2064 (1979)

[38]F.T.Arecchi, E.Courtens, pra V2, 1730 (1970)

[39]R.Bonifacio, P.Schwendimann, F.Haake, pra V4, 302 (1971)

[40]R.Bonifacio, L.A.Lugiato, pra V12, 587 (1975)

[41]R.Bonifacio, L.A.Lugiato, pra V11, 1507 (1975)

[42]J.I.Levatter, S.C.Lin, **Applied Physics Letters**

V25, 703 (1974)
[43]H.M.von Bergmann, V.Hasson, J.Brink, Optics Communications V18, 180 (1976)
[44]J.T.Lue, IEEE Transactions on Instrumentation and Measurement IM-34, 436 (1985)
[45]N.A.Kurnit, S.J.Tubbs, K.Bidhichand, L.W.Ryan, A.Javan, IEEE J Quantum Electronics QE-11, 174 (1975)
[46]A.W.Ali, Applied Optics V8, 993 (1969)
[47]V.Hasson, H.M.von Bergmann, J Physics E V9, 73 (1976)
[48]H.M. von Bergmann, J Physics E V10, 1210 (1977)
[49]V.Hasson,H.M.von Bergmann,D. Preussler, Applied Physics Letters V28, 17 (1976)
[50]O.P. Judd, Applied Physics Letters V22, 95 (1973)
[51]V.Hasson, D.Preussler, J.Klimek,H.M.von BergmannApplied Physics Letters V25,654 (1974)
[52]Principles of Radar,M.I.T. Radar School Staff, Eds. Reintjes, Coate, McGraw Hill,(1952)
[53]R.Targ,IEEE J Quantum Electronics QE 8, 726 (1972)
[54]M.Montaser Sabry, A. Hassan, M.Ewaida, J Physics E V17,103 (1984)